Published in final edited form as:
J Am Chem Soc. 2013 September 11; 135(36): 13222–13234. doi:10.1021/ja308229p.

Metal-organic Frameworks as A Tunable Platform for Designing Functional Molecular Materials

Cheng Wang[1,2,†], **Demin Liu**[1,†], and **Wenbin Lin**[1]

Wenbin Lin: wenbinlin@uchicago.edu

[1]Department of Chemistry, University of Chicago, 929 E. 57th Street, Chicago, IL 60637

[2]Department of Chemistry, CB#3290, University of North Carolina, Chapel Hill, NC, 27599, USA

Abstract

Metal-organic frameworks (MOFs), also known as coordination polymers, represent an interesting class of crystalline molecular materials that are synthesized by combining metal-connecting points and bridging ligands. The modular nature of and mild conditions for MOF synthesis have permitted the rational structural design of numerous MOFs and the incorporation of various functionalities via constituent building blocks. The resulting designer MOFs have shown promise for applications in a number of areas, including gas storage/separation, nonlinear optics/ferroelectricity, catalysis, energy conversion/storage, chemical sensing, biomedical imaging, and drug delivery. The structure-property relationships of MOFs can also be readily established by taking advantage of the knowledge of their detailed atomic structures, which enables fine-tuning of their functionalities for desired applications. Through the combination of molecular synthesis and crystal engineering MOFs thus present an unprecedented opportunity for the rational and precise design of functional materials.

Metal-organic frameworks (MOFs), also known as coordination polymers or coordination networks,[1] are crystalline materials built from metal ions or clusters bridged by organic linkers to form one-, two-, or three-dimensional structures. With Prussian blue[2] and metal phosphonates[3] as their prototypes, coordination polymers were well documented in the inorganic chemistry literature in the last century.[4] Yet this field had remained relatively unexplored, primarily due to the difficulty typically encountered in growing large single crystals of coordination polymers that are suitable for X-ray diffraction studies and the lack of easy-to-use computer programs for visualizing complicated structures of most coordination polymers. Robson and co-workers revitalized the field of coordination polymers by reporting the synthesis, X-ray structural characterization, and early topological analysis of coordination polymers built from Cu(I), Zn(II), Cd(II) metal-connecting points and cyano- or nitrile-bridging ligands in a series of seminal papers in 1989 and the early 1990s.[5] Shortly after Robson's papers, a number of research groups, including Fujita, Yaghi, Zaworotko, Kitagawa, Moore/Lee, and Férey, reported the synthesis and characterization of a large number of coordination polymers/MOFs built from many different metal-connecting points and bridging ligands.[6]

Based on the early topological studies by Robson and coworkers, Yaghi, O'Keeffe, and co-workers carried out systematic synthesis and topological analysis of porous MOFs, demonstrated the zeolitic properties of MOFs, and popularized the concepts of secondary building units (SBUs) and reticular nature of many MOFs.[7] Permanent porosity of MOFs

Correspondence to: Wenbin Lin, wenbinlin@uchicago.edu.

†These authors contributed equally.

was demonstrated by Kitagawa et al. and Yaghi et al., who used pyridine- and carboxylate-based bridging ligands in 1997 and 1998, respectively.[6g,8] Yaghi and co-workers were the first to realize the potential of using porous MOFs as storage materials for technologically important gaseous molecules, such as methane, hydrogen, and carbon dioxide.[6g,6h] Parallel to the ongoing work of Yaghi and O'Keeffe, in 1997 the Lin group initiated a research program that used MOFs as a platform to incorporate molecular functionalities into solid materials. Distinct from traditional inorganic materials, MOFs can be synthesized from well-defined molecular building blocks thanks to both the reliability of molecular synthesis and the hierarchical organization via crystal engineering. The first isoreticular MOFs were rationally designed based on 3-D diamondoid networks and 2-D grid structures by using systematically elongated pyridinecarboxylate ligands.[9] Second-order nonlinear optical properties were observed in the constructed MOFs, a result of the intrinsic electronic and structural asymmetry of pyridinecarboxylate building blocks.

Since these early studies, the MOF field has witnessed explosive growth in the past decade. Many research groups around the world have contributed to various aspects of MOFs, exploring their applications in many fields such as gas storage/seperation,[6h,10] nonlinear optics,[9e,9f] ferroelectricity,[11], conductivity/semiconductivity,[12] magnetism,[13] luminescence,[14] chemical sensing,[14b,15] catalysis,[16] biomedical imaging,[17] drug delivery,[18] and solar energy harvesting (Fig. 1).[19] In this paper, we discuss the rational design of functional molecular materials based on MOFs. We illustrate strategies for using MOFs as a highly versatile and tunable platform to incorporate diverse functionalities into molecular materials. Selected applications are highlighted in order to convey the enormous potential of MOFs as functional molecular materials.

Porous MOFs for Gas Storage and Separation

Following the seminal work by Yaghi et al. on hydrogen uptake by MOF-**5**, MOFs have been extensively studied in the past decade as hydrogen storage materials.[20] Suh and coworkers list in a recent review approximately 200 MOFs that have been carefully examined for hydrogen storage. Judicious selection of molecular building blocks can tune the framework connectivity, pore size, and surface area of a MOF in order to optimize its hydrogen sorption capacity. Typically, the weight% H_2 uptake capacity at 77 K tend to increase as the surface area of a MOF increases;[21] the volumetric H_2 storage capacity, however, does not usually benefit from high surface area because such a MOF tends to exhibit low density. The highest excess H_2 uptake capacity by weight% was reported by Hupp and coworkers for NU-100 at 9.95 wt% at 77 K and 56 bar.[21b] The highest total H_2 uptake capacity by weight% was reported by Yaghi and coworkers for MOF-210 at 17.6 wt % at 77 K and 80 bar.[21c] These values compare favorably with other materials, but are still short of US Department of Energy's 2015 target of system deliverable hydrogen over 5.5wt % and 40 g/L with a storage temperature no lower than −40 °C and a storage pressure no higher than 150 bar·· High volumetric hydrogen storage capacity is the most critical metric for practical hydrogen fueling in vehicles. Therefore, different strategies that deviate from simply pursuing ultrahigh specific surface areas need to be explored in order to achieve practically useful volumetric hydrogen uptake capacities.

A large MOF cavity does not effectively contribute to excess hydrogen uptake because of the lack of interactions between the framework and hydrogen molecules in the middle of the cavity. The cavity volume will reduce the denominator in a weight% uptake calculation, but will not contribute to hydrogen storage capacity in a volumetric uptake calculation. An ideal hydrogen uptake material should have pore size large enough for the ready access of hydrogen molecules without wasting pore volume, in order to maximize the physical interactions between the adsorbate and the porous material. The optimal performance at

room temperature for MOFs requires an H_2 adsorption isosteric heat of 15 kJ mol^{-1},[27] which is significantly higher than the observed isosteric heat of 5–12 kJ mol^{-1} for the majority of MOFs.[10d] Increasing H_2-framework interactions thus presents a major challenge and bottleneck for MOFs to store hydrogen in a practical manner. Creating open metal sites in MOFs has been shown to effectively increase these interactions, but impurities in hydrogen (such as water and nitrogen) could potentially poison these strongly adsorbing sites. Great progress has been made in designing MOFs for hydrogen storage in the past decade, and future efforts should be focused on increasing volumetric hydrogen uptake as well as enhancing the framework–hydrogen interactions.

As the principal component of natural gas, methane is both cleaner and more abundant than gasoline for large-scale transportation applications. A key hurdle for methane-based transportation lies in the lack of safe, cheap, and convenient means for methane storage, for which MOFs have recently shown great potential. A number of research groups are actively pursuing this topic.[21c,22] Table 1 lists several MOFs with the highest methane uptake capacity. The 6,8-connected Zn-TBCPPM MOF based on the tetrakis {3,5-bis[(4-carboxyl)phenyl]phenyl}methane (TBCPPM) bridging ligand shows an exceptionally high gas uptake capacity at 298 K with an excess CH_4 uptake of 17.5 wt% at 35 bar and 27.6 wt % at 80 bar.[23] Unlike hydrogen, the interactions between methane and the aromatic MOF frameworks are strong enough for practical storage applications.[21c] Rigorous investigation toward highly robust and affordable MOFs for large scale on-vehicle methane storage is urgently needed.

Since fossil fuels continue to represent the dominant source of energy production in the near future, the CO_2 level in the Earth atmosphere will further increase. One logical option to curtail the frightening rise of these levels is the capture of CO_2 from power generation sources. Although chemisorption of CO_2 by an amine solution is the industrial standard for CO_2 removal, amine degradation and the energy-intensive regeneration process are currently motivating researchers to explore alternative approaches. Solid adsorbents are advantageous because of their low heat capacities. The most widely used solid sorbents for CO_2 separation are zeolites due to their stability and well-defined structures. In recent years MOFs have attracted great attention as porous solids for CO_2 separation. Long and coworkers published a recent review of the CO_2 uptake capacities of MOFs.[24] CO_2 uptake values as high as 23.6 wt% at 0.1 atm and 35.2 wt% at 1 atm and 25 °C were obtained for Mg_2DOBDC (DOBDC: 2,5-dioxido-1,4-benzenedicarboxylate).[25] Respectable uptake values were also reported at lower CO_2 partial pressures; at 25 °C, mmen-Mg_2DOBPDC (mmen= N,N'-dimethylethylenediamine; DOBPDC = 4,4′-dioxido-3,3′-biphenyldicarboxylate) exhibited a CO_2 uptake of 8.1 wt% at 0.39 mbar and 10.3 wt% at 5 mbar.[26] It is reasonable to expect much higher CO_2 uptake capacities can be obtained for MOFs with optimum pore sizes, dangling functional groups, and open metal sites. Interactions between CO_2 and MOF frameworks are also much stronger than that between hydrogen and MOF frameworks, but MOFs' uptake capacities are not much higher than other classes of materials, particularly on a per volume basis.[28] Other issues that limit the use of MOFs as practical gas storage materials include moisture, thermal, and mechanical stability, scalable synthesis, and the availability of cheap metal sources and bridging ligands.

Although the majority of efforts over the past decade have focused on gas storage applications, MOFs have recently emerged as excellent candidate materials for gas separations.[10e] A large number of MOFs have been shown to selectively adsorb certain gas molecules, some of which have showed promising ability in the separation of gas mixtures.[32] Researchers have also successfully modified the structures and pore properties of MOFs at the molecular level in order to improve their selective adsorption and separation performance.[33] For example, Long and co-workers used Fe_2(DOBDC) to separate ethylene/

ethane and propylene/propane mixtures at 318 K. Both breakthrough data and simulation results demonstrate the high selectivity of the material as well as its capacity for the separation of hydrocarbons (Fig. 2).[34]

Thermal, chemical, and framework stability are crucial to the practical application of MOFs in gas separations. Indeed, separating gas mixture involves more variables than most laboratory-scale evaluations, which makes close collaboration between chemists, chemical engineers, and computer modeling scientists all the more important. For instance, in the case of CO_2 separation from flue gases, the partial pressure of CO_2 is very low, and the stream has a high temperature and contains water and other gases that can potentially poison the MOF binding sites. Survival and performance of MOFs under these conditions awaits investigation. Lastly, the ability to engineer large pore sizes with exquisite functionalities enables further potential of MOFs in separating mixtures that are not amenable to traditional inorganic porous materials, such as liquid/liquid separation[35] and enantioselective separation.[36] The bright future of MOFs in gas storage and separation applications depends largely on the participation of scientists and engineers across disciplines in order to make MOF-based gas storage and separation a reality.

Symmetry-breaking MOFs for Second Harmonic Generation and Ferroelectricity

Lin et al. first envisioned that MOFs provide an ideal platform for the design of functional materials whose physical properties depend on the internal symmetry of MOF crystals. Second harmonic generation (SHG), in which two photons are combined to generate a new one with twice the frequency, is highly dependent on crystal symmetry. SHG materials have widespread applications in laser devices and optical communication technologies. In order to meet the basic symmetry requirement, an SHG-active material must lack a center of symmetry. Lin et al. demonstrated that noncentrosymmetric MOFs can be rationally designed and synthesized by taking advantage of metal centers with well-defined geometry and highly directional metal-ligand coordination bonds.[9e,9f]

The diamondoid network represents one of the most reliable topological motifs for designing noncentrosytmmetric structures.[9b,9e] Although the diamond crystal (A4) itself crystallizes in the centrosymmetric space group $Fd\bar{3}m$ as a result of inversion centers that reside in the middle of the C-C linkages between adjacent nodes, the center of symmetry can be eliminated by connecting the tetrahedral nodes with unsymmetrical bridging ligands. Noncentrosymmetric MOFs of the diamondoid topology were rationally synthesized using unsymmetrical linear bridging ligands (such as *p*-pyridinecarboxylate) and tetrahedral metal centers (such as Zn^{2+} and Cd^{2+}) (Fig 3a).[9b,9d] In addition to breaking the center of symmetry in MOFs, the unsymmetrical nature of the bridging ligands also introduces electronic asymmetry and high hyperpolarizability, which is key to high SHG signals. Hydro(solvo)thermal reactions between $Zn(ClO_4)_2$ or $Cd(ClO_4)_2$ and the corresponding precursors of *p*pyridinecarboxylate ligands (Fig 3b) afforded a series of isoreticular MOFs of diamondoid topology with systematically elongated linear spacers (Fig 3c).[9b,9d] Each diamondoid network in these MOFs is intrinsically noncentrosymmetric because its building blocks lack the center of symmetry. However, as a *p*pyridinecarboxylate ligand becomes longer, the void space within a single diamondoid network gets larger to allow for multiple diamondoid networks to interpenetrate to fill the void space.[9e] Such framework interpenetration can potentially result in centrosymmetric MOFs as pairs of diamondoid networks may be related to each other by inversion centers. The degree of framework interpenetration can be controlled by adjusting ligand length in this archetypical series of isoreticular MOFs. The very difficult task of crystal engineering of noncentrosymmetric solids is thus reduced to a simple choice of *p*-pyridinecarboxylate ligands of appropriate

length. Importantly, the noncentrosymmetric diamondoid MOFs exhibited impressive SHG activities that correlate with the length of bridging ligand. The longer the bridge, the higher the SHG activity due to increased hyperpolarizability. The SHG properties of MOFs built from the longest ligands are comparable to that of the technologically important lithium niobate. The rational synthesis of noncentrosymmetric MOFs has provided the first example of MOF-based functional materials designed via a combination of molecular and crystal engineering.[9b,9d]

The modular synthetic nature of MOFs has enabled the synthesis of numerous SHG-active materials.[9b,9e,9f,37] With contributions from many researchers worldwide during the past decade, MOFs have undoubtedly emerged as a great platform for the design of noncentrosymmetric solids with SHG properties.[9f] Future efforts are needed to evaluate other key attributes of MOFs, such as chemical stability, mechanical strength, optical transparency, and phase-matchability, in order to move these scientific discoveries into their potential technological applications in electro-optic devices.

Similar symmetry principles were later adopted by Xiong, Cheetham, and others to design ferroelectric MOFs.[11b,38] Ferroelectric materials exhibit spontaneous electric polarization whose direction can be reversed by an electric field. This phenomenon can be used in random access memories, field-effect transistors, dielectric resonators, and filters for microwave communications, piezoelectric sensors and fast displays in electronic equipment. Ferroelectric crystals must crystallize in space groups belonging to the 10 polar point groups, C_1, C_s, C_2, C_{2v}, C_3, C_{3v}, C_4, C_{4v}, C_6, and C_{6v}. Several MOFs have been shown to be ferroelectric.[39]

Ferroelectricity was observed in $[Mn_3(HCO_2)_6](C_2H_5OH)$, in which ordering of the included ethanol molecules results in net polarization.[39a] Similarly, freezing disordered $Me_2NH_2^+$ cations in the negatively charged $[M(HCO_2)3]^-$ (M = Mn, Fe, Co, Ni, Zn) triggers the paraelectric-antiferroelectric transition.[11a] Changing the cation in the cavity to NH_4^+ led to paraelectric-ferroelectric transitions.[39b] Ferroelectric MOFs were also prepared using chiral bridging ligands. The Cd-TBP [TBP = N-(4-(tetrazol-5-yl)benzyl)proline] MOF exhibits a remnant polarization of 0.38 μC/cm^2 and coercive field of ca. 2.10 kV/cm (Fig. 3d and 3e).[39c] Several other homochiral MOFs have been reported to be ferroelectric,[11b] but all exhibited modest remnant polarization (0.25–0.90 μC/cm^2) and coercive fields (0.2–2.1 kV/cm).

Although synthesis of ferroelectric MOFs has been achieved, we have yet to develop rational strategies to control spontaneous electric polarization, via order-disorder symmetry breaking or displacement of ions, in order to move from serendipitous discoveries towards ferroelectric engineering. Given the ultimate goal of building functional devices, the mechanical stability of MOFs will require significant improvements. Methods for preparing high-quality single-crystalline MOF thin films are also needed to enable device fabrication.

Chiral MOFs as Single-Site Solid Asymmetric Catalysts

Heterogeneous catalysis with inorganic porous materials such as zeolites is of paramount importance for many industrial chemical processes. With the ability to assemble well-defined molecular building blocks into solid materials, MOFs are particularly suited to generating single-site solid catalysts with unprecedentedly uniform catalytic sites and open channels for shape-, size-, chemo-, and stereo-selective reactions. The molecular origin of the catalysts significantly broadens the scope of reactions that porous solids can successfully catalyze, and allows for the systematic tuning of catalytic activities. On the other hand, MOF-based solid catalysts can simply be recovered and reused, yielding reductions in cost of catalyst regeneration and product purification in industrial processes. Despite extensive

investigation into catalysis based on the connecting nodes of MOFs as Lewis acid,[6d,16e] its relatively high expense together with typically limited thermal and hydrolytic stabilities of MOFs make them unlikely candidates for catalyzing traditional industrial processes where historically zeolites have excelled as heterogeneous catalysts.[40]

Chiral MOFs are unmatched by zeolites in asymmetric catalysis.[41] Kim et al. first reported asymmetric catalysis using a chiral MOF in 2000, albeit at 8% enantiomeric excess (ee).[16a] In parallel, Lin et al. explored the construction of MOFs from chiral bridging ligands based on BINOL or BINAP derivatives, and disclosed catalytically active chiral MOFs with lanthanide metal-connecting points in 2001.[42] The first chiral MOF capable of catalyzing highly enantioselective reactions was reported in 2005.[16b, 43] The MOF was built from (*R*)-BINOL-bipyridine ligand and Cd^{2+} metal nodes, and upon treatment with $Ti(O^iPr)_4$, catalyzed asymmetric diethylzinc addition to aromatic aldehydes with up to 94% ee. Numerous chiral MOFs have since been constructed from enantiopure building blocks, and many of them serve as effective catalysts for a range of asymmetric organic transformations.[44] Significant progress has also been made in understanding the fundamentals of chiral MOF-catalyzed asymmetric reactions.[16f,45]

Effective chiral MOF catalysts must possess large open channels in order to transport organic substrates and products that are typically very large. This presents a significant challenge in part because MOFs built from elongated bridging ligands tend to form interpenetrated structures, which reduces or even eliminates the interior void space of the MOFs. Several methods, including tuning reaction temperatures or reagent concentrations, introducing bulky groups onto bridging ligands, or templating with bulky guest molecules, have recently been used to reduce/avoid framework interpenetration in achiral MOFs.[6h,46] Framework interpenetration in chiral MOFs can also be controlled using solvents of different sizes.[45f] Isoreticular chiral MOFs of the **pcu** topology were constructed from $[Zn_4(\mu_4\text{−}O)(O_2CR)_6]$ SBUs and systematically elongated chiral Mn-Salen derived dicarboxylate struts.[45f] These combinations yielded both noninterpenetrated and interpenetrated MOFs, depending on the sizes of the solvent molecules used for solvothermal crystal growth. This result points to templating effects of the solvent molecules. A similar strategy was used in the synthesis of a pair of catenation isomers of chiral MOFs built from $[Zn_4(\mu_4\text{-}O)(O_2CR)_6]$ SBUs and a redox-active Ru-Salen derived dicarboxylate strut.[47] This pair of CMOFs showed the first example of reversible single-crystal to single-crystal reduction/re-oxidation behaviors, allowing the transformation of catalytically-inactive Ru^{III}-based MOFs to active Ru^{II}-based MOF catalysts for the asymmetric cyclopropanation of styrene. The catalytic activity of Ru-Salen MOFs is highly catenation-dependent: the non-interpenetrated MOF is highly active while the interpenetrated MOF is nearly inactive owing to its inability to transport substrates through the small channels.

MOFs with large open channels tend to undergo significant framework distortion upon the removal of solvent molecules, a phenomenon known as breathing.[48] MOF breathing can alter the open channel sizes and shapes, which not only presents a significant challenge for MOF characterization, but also adversely impacts MOF catalytic performance. Recently, two catalyst activation processes have been used to minimize MOF breathing. Hupp et al. used supercritical CO_2 drying to remove solvents from MOF channels,[49] whereas Lin et al. used a freeze-drying method to remove solvent molecules from MOFs.[10b] In both drying processes, the surface tension of the solvent was reduced in order to minimize framework distortion in MOFs.

Regardless what types of activation methods are used, MOFs with extremely large channels inevitably undergo structural distortion when the included solvent molecules are removed.

As asymmetric catalysis is typically carried out in solution, the presence of large channels in MOFs is more appropriately ascertained by assaying the uptake of surrogate dye molecules in the presence of solvent molecules. A dye-uptake assay was developed to quantify the intrinsic porosity as well as the capability of the channels to transport large molecules in MOFs.[16f]

Substrate and product diffusion through MOF channels is another critical parameter for MOF catalysis. Lin et al. quantitatively determined molecular diffusion coefficients in solvent-filled MOF channels for the first time. By monitoring luminescence quenching as a result of quencher diffusion into MOFs,[50] Lin and co-workers probed the dynamics of amine diffusion into a MOF built from the $Ru(bpy)_3^{2+}$–derived bridging ligand. Modeling of time-dependent luminescence quenching data provided quantitative diffusion coefficients for the amine quenchers.

With increased understanding of MOF structures and dynamics, systematic studies were carried out to grasp the relationships between MOF open channel sizes and their catalytic activities/stereoselectivities using isoreticular MOFs with tunable pore and channel sizes. A series of mesoporous chiral MOFs with the framework formula $[(BINOL\text{-}TC)Cu_2(solvent)_2]$ (where BINOL-TCs are BINOL-based tetracarboxylate ligands) possess the same structures but different channel sizes (Fig. 4).[16f] Chiral Lewis acid catalysts were generated by post-synthesis functionalization with $Ti(O^iPr)_4$, and the resulting materials were highly active asymmetric catalysts for diethylzinc and alkynylzinc additions, which converted aromatic aldehydes into chiral secondary alcohols (Fig. 4c). The ee's of these reactions are highly dependent on the size of the channels, which determines the diffusion rates of organic substrates. In diethylzinc addition reactions to benzaldehyde, $[(BINOL\text{-}TC)Cu_2(solvent)_2]$ with the shortest ligand gave <3% ee, presumably as a result of the small channel size that cannot accommodate both benzaldehyde and diethylzinc reagents. The 1-phenyl-1-propanol product mostly resulted from the background reaction and is thus essentially racemic. As the open channel sizes increase, the ee's of the diethylzinc addition reactions increase to 70%, 82%, and 84%, respectively. The correlation between ee and open channel size in this series demonstrates the important role of substrate diffusion in MOF-catalyzed reactions.

Following the work of Hupp, Nguyen, and coworkers,[16c] isoreticular chiral Mn-Salen MOFs were used to catalyze asymmetric epoxidation of a variety of olefins with up to 92% ee.[45f] The open channel and pore sizes of these MOFs vary systematically owing to the tunable dicarboxylate struts and controllable interpenetration patterns. The conversion rates of these MOF-catalyzed reactions increase in the order of increasing open channel sizes in this series. It is also notable that the MOFs with the largest channel sizes gave a comparable conversion rate as the homogeneous catalyst, indicating that the catalytic activity of Chiral MOFs with large open channels is limited by intrinsic reactivity of the catalytic molecular building blocks.

MOFs also provide an ideal platform to incorporate multiple functionalities in a structurally ordered fashion. MOFs containing disparate catalytic centers can be constructed and used to catalyze a series of reactions in a tandem manner, leading to atom-economic chemical transformations. A chiral MOF built from the Mn–Salen derived dicarboxylic acid and a distorted $[Zn_4(\mu_4{-}O)(O_2CR)_6]$ SBU catalyzes sequential alkene epoxidation (by the Mn-Salen strut) and epoxide ring-opening reactions (by the $[Zn_4(\mu_4{-}O)(O_2CR)_6]$ SBU) in a highly regio- and stereo-selective manner (Fig. 5).[16g]

Asymmetric catalysis using chiral MOFs has witnessed tremendous progress in the past decade. It has become clear that chiral MOFs warrant further development into potentially practical catalysts for the production of optically pure organic molecules. The ability to

obtain high precision structural information of MOF-derived catalysts via single-crystal-to-single-crystal transformations provides a powerful tool to shed new light on important catalytic reactions.[45e] Further advancements in synthetic strategies, physical characterization, and catalytic processes are needed in order to move chiral MOF catalysts from curiosity-driven discoveries to practical applications.

Electro- and Photo-active MOFs for Energy Conversion and Storage

Porous and conductive materials are in great need for energy conversion and storage applications, as electrodes and electrocatalysts as well as key components in batteries, capacitors, and fuel cell membranes.[51] High surface area and conductive materials have recently been prepared using nanoscale materials, such as silicon nanotube arrays,[52] carbon nanotubes, and graphene.[53] MOFs present an interesting alternative to design porous and conductive materials.

Porous and electrically conductive MOFs with tunable functionalities can open doors to a variety of applications in energy conversion and storage. Despite their significance, electrically conductive porous MOFs remain under-explored.[54] The fundamental physics of electrically conductive materials with intrinsic porosity remain largely unknown but is worthy of significant research efforts.

Sulfur-based bridging ligands form strong interactions with metal ions, and can overcome the insulating nature of less covalent metal-ligand connections in typical MOFs. Multi-thiobenzene based ligands have been used to coordinate with different metal ions to form a number of semiconducting coordination polymers.[55] Kitagawa, H. et al. reported the first porous and conductive MOF from Cu(II) and pdt (pdt = 2,3-pyrazinedithiolate) building blocks through both Cu-S and Cu-N bonds in 2008.[56] This MOF showed a conductivity of 6×10^{-4} S/cm at 300 K, which was attributed to a bistability between $Cu_I[Cu^{III}(pdt)_2]$ and $Cu^{II}[Cu^{II}(pdt)_2]$ states. The isostructural $Cu[Ni(pdt)_2]$ MOF exhibited a BET surface area of 385 m^2/g.[12a] A conductivity of 1×10^{-4} S/cm was measured upon partial oxidation of this MOF by I_2, representing a 10^4 fold increase over the as-synthesized MOF. Interestingly, a conductive MOF was recently constructed from 1,2,3-triazole ligand and Fe^{2+} ions.[12c] This MOF exhibits a BET surface area of 450 m^2/g, and a conductivity of 1.0×10^{-3} S/cm upon I_2 oxidation.

Stacking of redox-active molecules was also exploited to construct porous and conductive MOFs, inspired by a large body of literature on semiconducting to conducting behaviors of charge transfer salts such as TTF-TCNQ (TTF = tetrathiafulvalene, TCNQ = tetracyanoquiondimethane) and their coordination polymer counterparts.[57] Several groups used TTF-derived tetracarboxylic acids (TTF-TC) to construct conductive MOFs. 3D-structures constructed from TTF-TC and alkaline cations were reported to have a conductivity of 1×10^{-3} S/cm at room temperature.[58] Dincă and coworkers recently reported the synthesis of a porous and conductive MOF using an expanded TTF-TC ligand, Zn_2(TTFTB), with a surface area of 662 m^2/g and a charge mobility of 0.2 $cm^2/V{\cdot}s$, a value comparable to or higher than most organic conductive polymers (Fig. 6).[12d]

In contrast to the scarcity of electrically conductive MOFs, a large number of MOFs have been examined for their ionic conductivities. Prussian Blue analogs have been intensively investigated as Li^+ conductors for potential applications in Li ion batteries.[59] Long et al. recently reported a Li^+ conductive MOF via addition of lithium isopropoxide to a MOF with open metal sites.[60] Proton conductivities of inorganic or organic compounds, such as zirconium phosphate, metal oxides, and Nafion, have been studied for applications in fuel cells and sensors.[61] MOFs provide a potential platform to fine-tune proton conductivity inside their channels.[6263] Over the past few years, several elegant strategies have been

developed to construct proton conductive MOFs: researchers have introduced acidic guest molecules such as water molecules in the voids, via assembling proton-containing anions such as NH_4^+, H_3O^+ and HSO_4^- in the channel, and by attaching acid groups on the framework. Proton conductivities as high as 10^{-2} S/cm have been achieved with MOFs. Performance of proton conductive MOFs has been tested under different humidity levels and working temperatures. For example, Shimizu and coworkers incorporated a MOF constructed from Na^+ and 2,4,6-trihydroxy-1,3,5-benzenetrisulfonate and partially loaded with 1*H*-1,2,4-triazole guests into a H_2/air membrane electrode assembly. The resulting membrane yielded an open circuit voltage of 1.18 V at 100 °C, corresponding to reversible thermodynamic potential within experimental errors.

MOFs have recently been examined in solar energy harvesting applications. Converting solar energy to chemical energy, as practiced by plants in natural photosynthesis for eons, requires three fundamental steps: sunlight absorption by antenna to create charge-separated excited states, creation of redox equivalents and their vectorial migration to reactive centers, and catalytic reactions to store chemical energy in the products using vectorially delivered electrons and holes.[64] Molecular systems capable of individual steps have been developed and extensively studied during the past several decades. However, these functional components need to be integrated into hierarchically organized structures in order to perform the ultimate task of solar energy harvesting. MOFs provide a versatile model system to integrate different functional components for solar energy conversion.

A phosphorescent MOF was constructed using $\{Ru[4,4'\text{-}(HO_2C)_2\text{-}bpy]_2bpy\}^{2+}$ as bridging ligands and Zn^{2+} as connecting nodes.[19a] The $Ru(bpy)_3^{2+}$ derivative in this MOF can be readily excited to its long-lived, triplet metal-to-ligand charge transfer (^{3}MLCT) excited state. The facile migration of the ^{3}MLCT excited states was demonstrated via Os doping by adding different amounts of $\{Os[4,4'\text{-}(HO_2C)_2\text{-}bpy]_2bpy\}^{2+}$ during crystal growth.[19a] Energy transfer dynamics in the MOF samples with 0, 0.3, 0.6, 1.4, and 2.6 mol% Os doping were carefully studied with a two-photon excitation at 850 nm (Fig. 7a). The Ru lifetime at 620 nm decreases from 171 ns in the pure Ru MOF to 29 ns in the sample with 2.6 mol % Os doping. In the mixed-metal MOFs, energy transfer was observed with an initial growth in Os emission corresponding to the decay of Ru excited states because of the Ru-to-Ru and Ru-to-Os energy transfers. Time-resolved luminescence studies demonstrated rapid, efficient energy migration in these isomorphous MOFs. Similar energy transfer processes were recently observed in porphyrin-based MOFs by Wiederrecht, Hupp, and co-workers.[65] The excited state migration in the framework was studied by site selective quenching whereas the migration rate and the reachable range of the excited state were deduced from the concentration dependent quenching data.

The light-harvesting ability of microscale MOFs was recently demonstrated via redox luminescence quenching (Fig 7b and c).[19b] Up to 98% emission quenching was achieved with either an oxidative quencher (1,4-benzoquinone, BQ) or a reductive quencher (N, N, N', N'-tetramethylbenzidine, TMBD), as a result of rapid energy migration over several hundred nanometers followed by efficient electron transfer quenching at the MOF/solution interface. The Stern-Vömer plots of these quenching processes were fitted to an equation based on a combination of static and diffusional quenching components. The rate constants for both quenching processes as well as association constants between the quenchers and the MOFs were obtained. These phosphorescent MOFs act as an excellent light-harvesting system by combining intra-framework energy migration and interfacial electron transfer quenching.

MOFs were also used to catalyze reactions that enable the conversion of solar energy to chemical energy. Catalytically competent Ir, Re, and Ru complexes with dicarboxylic acid

functionalities were incorporated into the $Zr_6O_4(OH)_4(bpdc)_6$ (UiO-67, bpdc = para-biphenyl-dicarboxylic acid) framework using a mix-and-match synthetic strategy.[19c] These MOFs exhibited high surface areas ranging from 1092 to 1497 m^2/g and are stable in acidic water. These MOFs were then used to catalyze water oxidation, CO_2 reduction, and organic transformations. Importantly, MOFs also provide a unique platform to study the mechanisms of molecular water oxidation reactions.[66]

Lin et al. recently demonstrated photocatalytic hydrogen production with Pt nanoparticle@phosphorescent MOF assemblies by taking advantage of the stability of UiO MOFs, light harvesting ability of phosphorescent MOFs, and the ability to assemble multiple functional components using the MOF platform.[67] Pt nanoparticles of 2–3 nm and 5–6 nm in diameter were selectively loaded onto channels of phosphorescent MOFs via MOF-mediated photoreduction of K_2PtCl_4. The resulting Pt@MOF assemblies served as effective photocatalysts for hydrogen evolution through the synergistic photo-excitation of the MOF frameworks and electron injection into the Pt nanoparticles. The Pt@MOF assembly gave a turnover number of 7000, approximately five times the value afforded by the homogeneous control, and could be readily recycled and reused by centrifugation.

MOFs have proved a promising platform for the assembly of multiple components for solar energy utilization. We envision that significant efforts will be devoted to developing photoactive, conductive, or redox-active MOFs for energy conversion and storage in the coming years. One major challenge in these MOF-based light-harvesting systems is the development of strategies to suppress recombination of the separated charge equivalents or the generated H_2 and O_2.

Responsive MOFs for Chemical Sensing

MOFs have been extensively explored as potential sensing materials.[15a,15b,15e,68] A number of research groups have designed MOFs as chemical sensors by taking advantage of the porous nature of MOFs and their luminescent properties.[14a] Nanoparticles of Eu-doped Gd MOF with the composition $Eu/Gd(bdc)_{1.5}(H_2O)_2$ were coated with a shell of silica in order to enhance their stability in water and to allow for functionalization with a silylated Tb-EDTA monoamide derivative.[69] The surface-grafted Tb-EDTA derivative binds dipycolylamine (DPA), a molecular marker in spore-producing bacteria, to turn on the Tb luminescence. The doped Eu^{3+} ions in the MOF served as an internal standard for the ratiometric luminescence sensing of spore-producing bacteria.

Chen and coworkers reported an Eu MOF with the formula $[Eu(pdc)_{1.5}(dmf)]\cdot(DMF)_{0.5}(H_2O)_{0.5}$ (pdc = pyridine-3,5-dicarboxylate), with free Lewis basic pyridyl sites for the sensing of metal ions.[68] The MOF emission, based on energy transfer from the pdc ligands to Eu^{3+} ions can be effectively quenched by different metal ions, due to the interruption of energy transfer when metal ions bind to the pyridyl moiety. The emission quenching can be quantitatively determined by Stern-VHJmer plot, which also serves as calibration curves for the quantitative determination of metal ion concentrations.

Lin et al. recently demonstrated oxygen sensing with MOFs built from phosphorescent Ir-complexes. The ^{3}MLCT emission of the MOF can be reversibly quenched by oxygen. Linear Stern-VHJmer plots of I_0/I vs. $p(O_2)$ (oxygen partial pressure) were obtained for these MOFs.[15d] Reversibility of the luminescent quenching was evaluated by examining the emission intensity change when the $p(O_2)$ was cycled between 0 and 0.1 atm. Permanent porosity was found to be necessary for kinetically reversible O_2 quenching because gas molecules need to freely diffuse inside the solids.

Li and coworkers reported luminescent detection of explosives using the $[Zn_2(bpdc)_2(bpee)]$ (bpee is 1,2-bipyridylethene) MOF.[15b] Thin films of the solvent-free MOF were prepared. The ligand centered luminescence of the MOF can be effectively quenched by trace amount of vapor of the solid explosives DNT and DMNB (Fig. 8).

Many practical sensing applications require extraordinarily high detection sensitivities. Amplified quenching is often exploited in order to enhance the detection sensitivity of many practical luminescence sensors.[70] Lin, Meyer, and coworkers demonstrated amplified quenching in phosphorescent MOFs that are composed of Ru(II)-(bpy) building blocks.[71] These MOFs showed up to 7000-fold enhancement of the Stern-VHJmer quenching constants in the presence of methyl viologen and methylene blue, as compared to a model complex. The amplified quenching was believed to result from strong non-covalent interactions between the MOF surface and cationic quencher molecules coupled with rapid energy transfer through the MOF microcrystals. Preconcentration of analytes in the MOF channels were also recently used to increase sensitivity of a chiral MOF in enantioselective sensing.[72]

Other properties of MOFs have also been exploited for sensing applications. For example, MOFs exhibit adsorbate-induced structural flexibility, known as “breathing effect”.[48] The large variation of volumes of some MOFs in the presence of adsorbate suggests a novel sensing mechanism: distortions in a MOF thin film can create stress at the interface with a second material. Allendorf and coworkers reported such a device constructed from HKUST-1 on a cantilever with a built-in piezoresistive sensor.[15a] The signal of molecular adsorption into the porous MOF can be efficiently converted to mechanical response, resulting in a reversible and selective sensor.

Spin-crossover is a phenomenon in which first row transition metal ions with d^4 to d^7 electronic configurations switch between states of high spin and low spin in response to external stimuli. This phenomenon can be used as a sensing modality. The nanoporous spin-crossover MOF $[Fe_2(azpy)_4(NCS)4]\cdot(guest)$ (azpy = trans-4,4’-azopyridine) exhibits reversible exchange of guest molecules which influences its spin transition properties. This solvent-induced spin-crossover provides a mechanism to detect the presence of guest molecules.[73] Several other groups have report similar systems.[74]

With their porous structures and ease of functionalization, MOFs are undoubtedly a promising class of materials for sensing applications. The sensitivity of MOF sensors can be enhanced using three strategies: thermodynamic and kinetic concentration enrichment of analytes in the pores, energy migration among the framework for amplified sensing, and cooperative interactions of the sensing moieties in a structurally regular material. The selectivity of MOF sensors can be achieved through the functionalization of the framework, particularly via orthogonal incorporation of different sensing motifs. However, for MOFs to work in a realistic sensing device, issues with chemical and mechanical stability and signal stability and reproducibility need to be addressed. A better understanding of analyte diffusion through MOF channels and control of MOF morphologies are also important. As many sensing applications will require MOF membranes, significant efforts to develop strategies for facile fabrication of uniform MOF films are urgently needed.

Nanoscale MOFs for Bio-Imaging and Cancer Therapy

Nanoparticles in the size range of 10–100 nm in diameter have been intensively studied as drug delivery vehicles and biomedical imaging agents. Such nanocarriers are particularly effective for cancer imaging and therapy due to the enhanced permeability and retention (EPR) effect that results from leaky vasculatures and ineffective lymphatic drainage in tumors.[75] Numerous preclinical studies suggest that nanoparticle-based cancer therapeutics

and diagnostic agents show enhanced efficacy and reduced side effects, owing to their unique physicochemical properties. The vast majority of nanocarriers can be categorized into either purely inorganic (such as quantum dots) or purely organic (such as liposomes). Nanoscale MOFs (NMOFs) have the potential to combine attractive features of both inorganic and organic nanocarriers, such as robust particle morphologies, compositional and structural diversity, and biodegradability, to provide a unique platform for delivering bio-imaging agents and cancer therapeutics.

Although countless examples of bulk MOFs have been reported, little was known about NMOFs prior to 2006.[76] Gd-BDC and Gd-BTC NMOFs were synthesized in reverse microemulsions.[17c,77] The particle morphologies can be reliably controlled and tuned by varying the water/surfactant molar ratio and reaction time. Several other techniques, including nanoprecipitation,[18b] solvothermal,[18c] and surfactant-templated solvothermal reactions[78] were subsequently developed to allow the synthesis of a variety of NMOFs that carry biomedically relevant agents either by direct incorporation[17b,17c] or by postsynthesis loading.[18a,18c,18g,79] In order to improve the NMOF stability and to impart biocompatibility and additional functionality, the surfaces of NMOFs have been modified with a thin shell of silica,[17b,17d,18b,80] organic polymers (e.g., polyethylene glycol, polyvinylpyrrolidone),[81] or lipid bilayers.[18e,18f] NMOF formulations with suitable surface properties for *in vitro* and *in vivo* applications are now undergoing preclinical testing.

NMOFs were first evaluated as contrast agents for magnetic resonance imaging (MRI). MRI is a non-invasive imaging technique wherein images are generated based on nuclear magnetic resonance (NMR) signals of water proton (^{1}H) nuclei in the specimen. MRI has excellent spatial resolution and depth of penetration, but suffers from low sensitivity. A relatively large dose of contrast agents is typically administered to provide adequate MR contrast. Researchers hypothesized that Gd NMOFs could carry large payloads of paramagnetic Gd^{3+} ions and should serve as excellent nanoparticulate contrast agents for MRI. Extraordinarily large longitudinal (r1) and transverse (r2) relaxivities on a per mM of nanoparticle basis were obtained for Gd-BDC and Gd-BTC NMOFs as a result of high payloads of Gd^{3+} centers carried by each particle. The MR relaxivities of these NMOFs are inversely dependent on their particle sizes, consistent with the higher surface-to-volume ratios for smaller NMOFs.[17b,78]

To circumvent Gd^{3+} toxicity, Mn NMOFs were recently examined as MRI contrast agents.[17b] $Mn(BDC)(H_2O)_2$ and $Mn(BTC)_2(H_2O)_6$ particles were synthesized and coated with a thin silica shell followed by functionalization with a cyclic arginine-glycine-aspartate (cRGD) peptide for cancer-specific targeting. The Mn NMOFs were shown *in vitro* to be highly efficient T_1-weighted MR contrast agents due to their ability to carry large a payload of Mn^{2+} ions, which were released upon NMOF dissolution. *In vitro* MRI, confocal microscopy, and ICP-MS studies confirmed the increased uptake of cRGD-targeted particles. Iron-based NMOFs of the MIL structures were shown to be efficient contrast agents for T_2-weighted MR imaging.[18a] The PEGylated MIL-88 nanoparticles exhibited an r2 relaxivity of 50 $mM^{-1}s^{-1}$ at 9.4 T. *In vivo* MR imaging of Wistar female rats 30 mins after nanoparticle injection showed enhanced contrast in the liver and spleen (Fig. 10). Complete clearance of these particles was observed after three months.

By incorporating high Z element building blocks, NMOFs have also been tested as contrast agents for X-ray computed tomography (CT) imaging.[17c] Iodinated NMOFs were prepared using 2,3,4,5,6-tetraiodo-1,4-benzenedicarboxylic acid (I_4-$BDCH_2$) as the bridging ligands and Cu^{2+} and Zn^{2+} as the metal-connecting points. The iodinated NMOFs carried very high iodine content (up to 63wt%). Phantom studies showed that these particles have X-ray attenuation coefficients comparable to that of the molecular contrast agent (Iodixanol). More

recently, NMOFs of the UiO-66 structure containing high Zr (37 wt%) and Hf (57 wt%) content were synthesized and characterized, and their potential as contrast agents for CT imaging was evaluated.[80a] Hf NMOFs were twice as efficient in attenuating X-rays as Iodixanol, resulting from higher X-ray attenuation coefficients of Hf compared to I. Hf-NMOFs of different sizes were coated with silica and poly(ethylene glycol) (PEG) in order to enhance biocompatibility, and were used for *in vivo* CT imaging of mice, showing increased attenuation in the liver and spleen.

Optical imaging (OI) is another powerful imaging modality for visualizing tumor and other diseased tissues. Two major types of OI probes are currently under intensive investigation: organic-dye loaded nanoparticles and luminescent quantum dots. The former suffer from self-quenching and photobleaching, while the latter have high toxicity. In contrast, luminescence originating from the triplet excited states of metal complexes tends to have long lifetimes and large Stokes shifts, and does not self-quench even at very high dye loadings. Phosphorescent NMOFs containing carboxylic acid derivative of $Ru(bpy)_3^{2+}$ were synthesized and contained very high $Ru(bpy)_3^{2+}$ dye loadings (up to 78.7%).[17d] The phosphorescent NMOFs were further stabilized with a thin shell of amorphous silica and functionalized with PEG and PEG-anisamide. Enhanced contrast and uptake was confirmed by laser scanning confocal fluorescence microscopy and particle uptake studies using H460 lung cancer cells.

A key challenge in cancer therapy is to deliver anticancer therapeutics selectively to tumors while minimizing accumulation in normal tissues. Nanocarrier-based delivery can overcome this challenge through the EPR effect to achieve differential drug accumulation in tumors vs. normal tissues.[82] NMOFs provide an intriguing platform for delivering cancer therapeutics because of their ability to carry exceptionally high payloads and their biodegradable nature.[18b,18c]

Lin et al. developed a NMOF formulation that carried 46.7 wt% cisplatin in 2008.[18b] Rapid addition of methanol to a solution of Tb^{3+} ions and *c,c,t*-(diamminedichlorodisuccinato)Pt(IV) resulted in an NMOF with the formula of $Tb_2(DSCP)_3(H_2O)_{12}$, which was coated with a thin layer of silica in order to prevent premature drug release. The thickness of the silica shell was further tuned to optimize the release rate of the Pt drugs in biologically relevant media. Surface modification with silyl-derived c(RGDfK) led to enhanced cellular uptake and a lower half maximal inhibitory concentration (IC_{50}) value compared to free cisplatin.

An iron-based NMOF was also developed for cisplatin delivery. 17.5 mol% of 2-aminoterephthalic acid (NH_2-BDC) was doped into crystalline Fe-BDC nanoparticles of the MIL-101 structure (Fig. 11).[18c] The amino groups were used for covalent attachment of Br-BODIPY (1,3,5,7-tetramethyl-4,4-difluoro-8-bromomethyl-4-bora-3a,4a-diaza-s-indacene) as an optical imaging contrast agent and the cisplatin prodrug c,c,t-$Pt(NH_3)_2Cl_2$(succinate)(OEt). These particles were further stabilized with a thin shell of silica and modified with the cRGD peptide to target human colon cancer cells. Lin et al. further refined platin delivery based on the NMOF strategy, and has demonstrated *in vivo* efficacy of a recent NMOF formulation of oxaliplatin analog against pancreatic cancer in mouse xenografts.[80b]

The NMOF particles can be readily formulated to deliver other important cancer therapeutics, including busulfan,[18a] methotrexate[18e] and nitrogen-containing bisphosphonates.[18f] In addition, MIL-based NMOFs have been used to deliver triphosphorylated azidothymidine for treating HIV-infected cells.[18a]

Despite their infancy, NMOFs have shown great promise as novel nanocarriers for imaging agents and chemotherapeutics. We foresee that many other imaging agents and drugs will be

incorporated into NMOFs in the future when researchers begin taking advantage of the mild conditions and the highly tunable nature of NMOF synthesis. The ability to combine targeting, drug release, molecular imaging, and therapeutic functions into a single NMOF particle will further facilitate cancer diagnosis and therapy. The use of nontoxic components, the endowment of stealth property to NMOFs, and a balance between MOF stability and controlled drug release are needed before NMOFs can be advanced to clinical use.

Concluding Remarks

After fifteen years of intense research activities on MOFs, the field has moved beyond the initial fascination with aesthetically pleasing MOF structures. An ever-increasing number of research groups are now exploring potential applications of MOFs. In particular, a plethora of MOFs with unprecedented porosity and which exhibit unmatched uptake capacities for small gaseous molecules are now available. The modular nature of MOF synthesis and the ease with which molecular functionalities can be incorporated into MOFs have led to numerous molecular materials for potential applications in other areas, such as nonlinear optics/ferroelectricity, asymmetric catalysis, energy conversion and storage, chemical sensing, bioimaging, and drug delivery. However, the potential of MOFs in some applications will be compromised by their relatively high costs and limited thermal and hydrolytic stabilities. In order to move MOFs from curiosity-driven discoveries to practical applications, close collaborations among scientists and engineers from many different disciplines are needed in order to critically assess the true potential of MOFs in each area. With key design principles developed in the past decade, MOFs will likely emerge as a unique class of molecular materials that will find real-world applications in the next decade.

Acknowledgments

We thank NSF (CHE-1111490) and NIH-NCI (U01-CA151455) for financial support. C.W. acknowledges the UNC Department of Chemistry for a Venable Award. S.F. Reichard, MA contributed editing.

REFERENCES

1. There is currently no consensus on the definitions of coordination polymer vs. metal-organic framework. In this perspective, we use the two terms synonymsly.
2. a) Itaya K, Uchida I, Neff VD. Acc. Chem. Res. 1986; 19:162.b) Entley WR, Girolami GS. Science. 1995; 268:397. [PubMed: 17746547] c) Ferlay S, Mallah T, Ouahes R, Veillet P, Verdaguer M. Nature. 1995; 378:701.d) Sato O, Iyoda T, Fujishima A, Hashimoto K. Science. 1996; 272:704. [PubMed: 8662564]
3. a) Clearfield A, Stynes JA. J. Inor. Nucl. Chem. 1964; 26:117.b) Clearfield A. Karlin KD. Progress in Inorganic Chemistry, Vol 47. 1998; Vol. 47:371.c) Guang C, Hong HG, Mallouk TE. Acc. Chem. Res. 1992; 25:420.d) Cheetham AK, Férey G, Loiseau T. Angew. Chem. Int. Ed. 1999; 38:3268.
4. a) Yukio Kinoshita IM, Taiichi Higuchi, Saito Yoshihiko. Bull. Chem. Soc. Japan. 1959; 32:1221.b) Yutaka, Osaki KN.; Watanabe, Tokunosuke. J. Phys. Soc. Japan. 1964; 19:717.c) Malard C, Pezerat H, Herpin P, Toledano P. J. Solid State Chem. 1982; 41:67.d) Weiss A, Riegler E, Alt I, Bohme H, Robl C. Z. Naturforsch. B. 1986; 41:18.
5. a) Abrahams BF, Hoskins BF, Robson R. J. Chem. Soc. -Chem. Commun. 1990:60.b) Gable RW, Hoskins BF, Robson R. J. Chem. Soc. -Chem. Commun. 1990:762.c) Hoskins BF, Robson R. J. Am. Chem. Soc. 1989; 111:5962.d) Hoskins BF, Robson R. J. Am. Chem. Soc. 1990; 112:1546.
6. a) Gardner GB, Venkataraman D, Moore JS, Lee S. Nature. 1995; 374:792.b) Kitagawa S, Matsuyama S, Munakata M, Emori T. J. Chem. Soc.-Dalton Trans. 1991:2869.c) Kitagawa S, Matsuyama S, Munakata M, Osawa N, Masuda H. J. Chem. Soc.-Dalton Trans. 1991:1717.d) Fujita M, Kwon YJ, Washizu S, Ogura K. J. Am. Chem. Soc. 1994; 116:1151.e) Yoshizawa M, Takeyama Y, Kusukawa T, Fujita M. Angew. Chem. Int. Ed. 2002; 41:1347.f) Yaghi OM, Li GM, Li HL. Nature. 1995; 378:703.g) Li H, Eddaoudi M, O'Keeffe M, Yaghi OM. Nature. 1999; 402:276.h) Eddaoudi M, Kim J, Rosi N, Vodak D, Wachter J, O'Keeffe M, Yaghi OM. Science. 2002; 295:469.

[PubMed: 11799235] i) Subramanian S, Zaworotko MJ. J. Chem. Soc. -Chem. Commun. 1993:952.j) Zaworotko MJ. Chem. Soc. Rev. 1994; 23:283.k) Riou D, Roubeau O, Férey G. Microporous Mesoporous Mater. 1998; 23:23.

7. a) O'Keeffe M, Eddaoudi M, Li HL, Reineke T, Yaghi OM. J. Solid State Chem. 2000; 152:3.b) Eddaoudi M, Moler DB, Li HL, Chen BL, Reineke TM, O'Keeffe M, Yaghi OM. Acc. Chem. Res. 2001; 34:319. [PubMed: 11308306] c) Kim J, Chen BL, Reineke TM, Li HL, Eddaoudi M, Moler DB, O'Keeffe M, Yaghi OM. J. Am. Chem. Soc. 2001; 123:8239. [PubMed: 11516275]
8. Kondo M, Yoshitomi T, Seki K, Matsuzaka H, Kitagawa S. Angew. Chem. Int. Ed. 1997; 36:1725.
9. a) Lin WB, Evans OR, Xiong RG, Wang ZY. J. Am. Chem. Soc. 1998; 120:13272.b) Evans OR, Xiong RG, Wang ZY, Wong GK, Lin WB. Angew. Chem. Int. Ed. 1999; 38:536.c) Evans OR, Lin WB. Chem. Mater. 2001; 13:3009.d) Evans OR, Lin WB. Chem. Mater. 2001; 13:2705.e) Evans OR, Lin W. Acc. Chem. Res. 2002; 35:511. [PubMed: 12118990] f) Wang C, Zhang T, Lin W. Chem. Rev. 2011; 112:1084. [PubMed: 22070202]
10. a) Rowsell JL, Yaghi OM. Angew. Chem. Int. Ed. 2005; 44:4670.b) Ma L, Jin A, Xie Z, Lin W. Angew. Chem. Int. Ed. 2009; 48:9905.c) Wang Z, Tanabe KK, Cohen SM. Chem. Eur. J. 2009; 16:212. [PubMed: 19918824] d) Suh MP, Park HJ, Prasad TK, Lim DW. Chem. Rev. 2012; 112:782. [PubMed: 22191516] e) Li JR, Sculley J, Zhou HC. Chem. Rev. 2012; 112:869. [PubMed: 21978134] f) Sumida K, Rogow DL, Mason JA, McDonald TM, Bloch ED, Herm ZR, Bae TH, Long JR. Chem. Rev. 2012; 112:724. [PubMed: 22204561]
11. a) Jain P, Ramachandran V, Clark RJ, Zhou HD, Toby BH, Dalal NS, Kroto HW, Cheetham AK. J. Am. Chem. Soc. 2009; 131:13625. [PubMed: 19725496] b) Zhang W, Xiong R-G. Chem. Rev. 2011; 112:1163. [PubMed: 21939288]
12. a) Kobayashi Y, Jacobs B, Allendorf MD, Long JR. Chem. Mater. 2010; 22:4120.b) Silva CG, Corma A, Garcia H. J. Mater. Chem. 2010; 20:3141.c) Gándara F, Uribe-Romo FJ, Britt DK, Furukawa H, Lei L, Cheng R, Duan X, O'Keeffe M, Yaghi OM. Chem. Eur. J. 2012; 18:10595. [PubMed: 22730149] d) Narayan TC, Miyakai T, Seki S, Dincă M. J. Am. Chem. Soc. 2012; 134:12932.
13. a) Kurmoo M. Chem. Soc. Rev. 2009; 38:1353. [PubMed: 19384442] b) Beltran LMC, Long JR. Acc. Chem. Res. 2005; 38:325. [PubMed: 15835879]
14. a) Ma L, Evans OR, Foxman BM, Lin W. Inor. Chem. 1999; 38:5837.b) Cui YJ, Yue YF, Qian GD, Chen BL. Chem. Rev. 2012; 112:1126. [PubMed: 21688849] c) Allendorf MD, Bauer CA, Bhakta RK, Houk RJT. Chem. Soc. Rev. 2009; 38:1330. [PubMed: 19384441]
15. a) Allendorf MD, Houk RJ, Andruszkiewicz L, Talin AA, Pikarsky J, Choudhury A, Gall KA, Hesketh PJ. J. Am. Chem. Soc. 2008; 130:14404. [PubMed: 18841964] b) Lan A, Li K, Wu H, Olson DH, Emge TJ, Ki W, Hong M, Li J. Angew. Chem. Int. Ed. 2009; 48:2334.c) White KA, Chengelis DA, Gogick KA, Stehman J, Rosi NL, Petoud S. J. Am. Chem. Soc. 2009; 131:18069. [PubMed: 19938832] d) Xie Z, Ma L, deKrafft KE, Jin A, Lin W. J. Am. Chem. Soc. 2010; 132:922. [PubMed: 20041656] e) Kreno LE, Leong K, Farha OK, Allendorf M, Van Duyne RP, Hupp JT. Chem. Rev. 2012; 112:1105. [PubMed: 22070233]
16. a) Seo JS, Whang D, Lee H, Jun SI, Oh J, Jeon YJ, Kim K. Nature. 2000; 404:982. [PubMed: 10801124] b) Wu CD, Hu A, Zhang L, Lin W. J. Am. Chem. Soc. 2005; 127:8940. [PubMed: 15969557] c) Cho SH, Ma B, Nguyen ST, Hupp JT, Albrecht-Schmitt TE. Chem. Commun. 2006:2563.d) Hasegawa S, Horike S, Matsuda R, Furukawa S, Mochizuki K, Kinoshita Y, Kitagawa S. J. Am. Chem. Soc. 2007; 129:2607. [PubMed: 17288419] e) Lee J, Farha OK, Roberts J, Scheidt KA, Nguyen ST, Hupp JT. Chem. Soc. Rev. 2009; 38:1450. [PubMed: 19384447] f) Ma L, Falkowski JM, Abney C, Lin W. Nat. Chem. 2010; 2:838. [PubMed: 20861899] g) Song F, Wang C, Lin W. Chem. Commun. 2011; 47:8256.
17. a) Rieter WJ, Taylor KML, An HY, Lin WL, Lin WB. J. Am. Chem. Soc. 2006; 128:9024. [PubMed: 16834362] b) Taylor KML, Rieter WJ, Lin W. J. Am. Chem. Soc. 2008; 130:14358. [PubMed: 18844356] c) deKrafft KE, Xie Z, Cao G, Tran S, Ma L, Zhou OZ, Lin W. Angew. Chem. Int. Ed. 2009; 48:9901.d) Liu D, Huxford RC, Lin W. Angew. Chem. Int. Ed. 2011; 50:3696.
18. a) Horcajada P, Chalati T, Serre C, Gillet B, Sebrie C, Baati T, Eubank JF, Heurtaux D, Clayette P, Kreuz C, Chang J-S, Hwang YK, Marsaud V, Bories P-N, Cynober L, Gil S, F900E9;rey G, Couvreur P, Gref R. Nat. Mater. 2010; 9:172. [PubMed: 20010827] b) Rieter WJ, Pott KM, Taylor

KM, Lin W. J. Am. Chem. Soc. 2008; 130:11584. [PubMed: 18686947] c) Taylor-Pashow KML, Rocca JD, Xie Z, Tran S, Lin W. J. Am. Chem. Soc. 2009; 131:14261. [PubMed: 19807179] d) Taylor-Pashow KML, Della Rocca J, Huxford RC, Lin WB. Chem. Commun. 2010; 46:5832.e) Huxford RC, deKrafft KE, Boyle WS, Liu D, Lin W. Chem. Sci. 2012; 3:198.f) Liu D, Kramer SA, Huxford-Phillips RC, Wang S, Della Rocca J, Lin W. Chem. Commun. 2012; 48:2668.g) Horcajada P, Serre C, Maurin G, Ramsahye NA, Balas F, Vallet-Regí Ma, Sebban M, Taulelle F, Férey Gr. J. Am. Chem. Soc. 2008; 130:6774. [PubMed: 18454528] h) Horcajada P, Gref R, Baati T, Allan PK, Maurin G, Couvreur P, Férey G, Morris RE, Serre C. Chem. Rev. 2011; 112:1232. [PubMed: 22168547]

19. a) Kent CA, Mehl BP, Ma L, Papanikolas JM, Meyer TJ, Lin W. J. Am. Chem. Soc. 2010; 132:12767. [PubMed: 20735124] b) Kent CA, Liu D, Ma L, Papanikolas JM, Meyer TJ, Lin W. J. Am. Chem. Soc. 2011; 133:12940. [PubMed: 21776996] c) Wang C, Xie Z, deKrafft KE, Lin W. J. Am. Chem. Soc. 2011; 133:13445. [PubMed: 21780787]
20. Rowsell JLC, Millward AR, Park KS, Yaghi OM. J. Am. Chem. Soc. 2004; 126:5666. [PubMed: 15125649]
21. a) Rowsell JLC, Spencer EC, Eckert J, Howard JAK, Yaghi OM. Science. 2005; 309:1350. [PubMed: 16123294] b) Farha OK, Özgür Yazaydın A, Eryazici I, Malliakas CD, Hauser BG, Kanatzidis MG, Nguyen ST, Snurr RQ, Hupp JT. Nat. Chem. 2010; 2:944. [PubMed: 20966950] c) Furukawa H, Ko N, Go YB, Aratani N, Choi SB, Choi E, Yazaydin AO, Snurr RQ, O'Keeffe M, Kim J, Yaghi OM. Science. 2010; 329:424. [PubMed: 20595583] d) An J, Farha OK, Hupp JT, Pohl E, Yeh JI, Rosi NL. Nat. Commun. 2012; 3:604. [PubMed: 22215079]
22. a) Tan C, Yang S, Champness NR, Lin X, Blake AJ, Lewis W, Schroder M. Chem. Commun. 2011; 47:4487.b) Guo Z, Wu H, Srinivas G, Zhou Y, Xiang S, Chen Z, Yang Y, Zhou W, O'Keeffe M, Chen B. Angew. Chem. Int. Ed. 2011; 50:3178.c) Ma S, Sun D, Simmons JM, Collier CD, Yuan D, Zhou H-C. J. Am. Chem. Soc. 2007; 130:1012. [PubMed: 18163628] d) Yuan D, Zhao D, Sun D, Zhou HC. Angew. Chem. Int. Ed. 2010; 49:5357.e) Li B, Zhang Z, Li Y, Yao K, Zhu Y, Deng Z, Yang F, Zhou X, Li G, Wu H, Nijem N, Chabal YJ, Lai Z, Han Y, Shi Z, Feng S, Li J. Angew. Chem. Int. Ed. 2012; 51:1412.f) Park HJ, Lim D-W, Yang WS, Oh T-R, Suh MP. Chem. Eur. J. 2011; 17:7251. [PubMed: 21560171] g) Han D, Jiang F-L, Wu M-Y, Chen L, Chen Q-H, Hong M-C. Chem. Commun. 2011; 47:9861.
23. Liu D, Wu H, Wang S, Xie Z, Li J, Lin W. Chem. Sci. 2012; 3:3032.
24. D'Alessandro DM, Smit B, Long JR. Angew. Chem. Int. Ed. 2010; 49:6058.
25. Caskey SR, Wong-Foy AG, Matzger AJ. J. Am. Chem. Soc. 2008; 130:10870. [PubMed: 18661979]
26. McDonald TM, Lee WR, Mason JA, Wiers BM, Hong CS, Long JR. J. Am. Chem. Soc. 2012; 134:7056. [PubMed: 22475173]
27. Bhatia SK, Myers AL. Langmuir. 2006; 22:1688. [PubMed: 16460092]
28. a) Walton KS, Abney MB, Douglas LeVan M. Microporous Mesoporous Mater. 2006; 91:78.b) Zhang J, Singh R, Webley PA. Microporous Mesoporous Mater. 2008; 111:478.
29. Rowsell JLC, Millward AR, Park KS, Yaghi OM. J. Am. Chem. Soc. 2004; 126:5666. [PubMed: 15125649]
30. Yan Y, Lin X, Yang S, Blake AJ, Dailly A, Champness NR, Hubberstey P, Schroder M. Chem. Commun. 2009:1025.
31. Dincă M, Dailly A, Liu Y, Brown CM, Neumann DA, Long JR. J. Am. Chem. Soc. 2006; 128:16876. [PubMed: 17177438]
32. a) Li J-R, Kuppler RJ, Zhou H-C. Chem. Soc. Rev. 2009; 38:1477. [PubMed: 19384449] b) Férey G, Serre C, Devic T, Maurin G, Jobic H, Llewellyn PL, De Weireld G, Vimont A, Daturi M, Chang J-S. Chem. Soc. Rev. 2011; 40:550. [PubMed: 21180728]
33. Mohideen MIH, Xiao B, Wheatley PS, McKinlay AC, Li Y, Slawin AMZ, Aldous DW, Cessford NF, Düren T, Zhao X, Gill R, Thomas KM, Griffin JM, Ashbrook SE, Morris RE. Nat. Chem. 2011; 3:304. [PubMed: 21430690]
34. Bloch ED, Queen WL, Krishna R, Zadrozny JM, Brown CM, Long JR. Science. 2012; 335:1606. [PubMed: 22461607]
35. Cychosz KA, Ahmad R, Matzger AJ. Chem. Sci. 2010; 1:293.

36. a) Liu Y, Xuan W, Cui Y. Adv. Mater. 2010; 22:4112. [PubMed: 20799372] b) Nuzhdin AL, Dybtsev DN, Bryliakov KP, Talsi EP, Fedin VP. J. Am. Chem. Soc. 2007; 129:12958. [PubMed: 17924635]
37. a) Evans OR, Wang ZY, Lin WB. Chem. Commun. 1999:1903.b) Lin WB, Wang ZY, Ma L. J. Am. Chem. Soc. 1999; 121:11249.
38. Rao CNR, Cheetham AK, Thirumurugan A. J. Phys. Condens. Matter. 2008; 20
39. a) Cui H, Wang Z, Takahashi K, Okano Y, Kobayashi H, Kobayashi A. J. Am. Chem. Soc. 2006; 128:15074. [PubMed: 17117843] b) Xu G-C, Zhang W, Ma X-M, Chen Y-H, Zhang L, Cai H-L, Wang Z-M, Xiong R-G, Gao S. J. Am. Chem. Soc. 2011; 133:14948. [PubMed: 21870842] c) Ye Q, Song Y-M, Wang G-X, Chen K, Fu D-W, Hong Chan PW, Zhu J-S, Huang SD, Xiong R-G. J. Am. Chem. Soc. 2006; 128:6554. [PubMed: 16704244]
40. Lin WB. J. Solid State Chem. 2005; 178:2486.
41. Sun JL, Bonneau C, Cantin A, Corma A, Diaz-Cabanas MJ, Moliner M, Zhang DL, Li MR, Zou XD. Nature. 2009; 458:1154. [PubMed: 19407798]
42. Evans OR, Ngo HL, Lin WB. J. Am. Chem. Soc. 2001; 123:10395. [PubMed: 11603994]
43. Highly enantioselective solid catalysts before 2005 were non-crystalline without well-defined crystal structures. See Hu A, Ngo HL, Lin W. Angew. Chem. Int. Ed. Engl. 2003; 42:6000. [PubMed: 14679554] Hu A, Ngo HL, Lin W. J. Am. Chem. Soc. 2003; 125:11490. [PubMed: 13129339]
44. a) Ma L, Abney C, Lin W. Chem. Soc. Rev. 2009; 38:1248. [PubMed: 19384436] b) Yoon M, Srirambalaji R, Kim K. Chem. Rev. 2012; 112:1196. [PubMed: 22084838]
45. a) Oxford GAE, Snurr RQ, Broadbelt LJ. Ind. Eng. Chem. Res. 2010; 49:10965.b) Wang C, Zheng M, Lin W. J. Phys. Chem. Lett. 2011; 2:1701.c) Zhang T, Song F, Lin W. Chem. Commun. 2012; 48:8766.d) Zheng M, Liu Y, Wang C, Liu S, Lin W. Chem. Sci. 2012; 3:2623.e) Ma L, Wu C-D, Wanderley MM, Lin W. Angew. Chem. Int. Ed. 2010; 49:8244.f) Song F, Wang C, Falkowski JM, Ma L, Lin W. J. Am. Chem. Soc. 2010; 132:15390. [PubMed: 20936862]
46. a) Zhang J, Wojtas L, Larsen RW, Eddaoudi M, Zaworotko MJ. J. Am. Chem. Soc. 2009; 131:17040. [PubMed: 19891485] b) Farha OK, Malliakas CD, Kanatzidis MG, Hupp JT. J. Am. Chem. Soc. 2009; 132:950. [PubMed: 20039671] c) Ma S, Sun D, Ambrogio M, Fillinger JA, Parkin S, Zhou HC. J. Am. Chem. Soc. 2007; 129:1858. [PubMed: 17256862]
47. Falkowski JM, Wang C, Liu S, Lin W. Angew. Chem. Int. Ed. 2011; 123:8833.
48. a) Serre C, Millange F, Thouvenot C, Nogues M, Marsolier G, Louer D, Férey G. J. Am. Chem. Soc. 2002; 124:13519. [PubMed: 12418906] b) Llewellyn PL, Maurin G, Devic T, Loera-Serna S, Rosenbach N, Serre C, Bourrelly S, Horcajada P, Filinchuk Y, Férey G. J. Am. Chem. Soc. 2008; 130:12808. [PubMed: 18729451] c) Férey G, Serre C. Chem. Soc. Rev. 2009; 38:1380. [PubMed: 19384443]
49. Nelson AP, Farha OK, Mulfort KL, Hupp JT. J. Am. Chem. Soc. 2009; 131:458. [PubMed: 19108683]
50. Wang C, Lin W. J. Am. Chem. Soc. 2011; 133:4232. [PubMed: 21384886]
51. a) Kondrat S, Perez CR, Presser V, Gogotsi Y, Kornyshev AA. Energy Env. Sci. 2012; 5:6474.b) Simon P, Gogotsi Y. Nat. Mater. 2008; 7:845. [PubMed: 18956000]
52. Hochbaum AI, Yang P. Chem. Rev. 2009; 110:527. [PubMed: 19817361]
53. Liang Y, Wang H, Diao P, Chang W, Hong G, Li Y, Gong M, Xie L, Zhou J, Wang J, Regier TZ, Wei F, Dai H. J. Am. Chem. Soc. 2012; 134:15849. [PubMed: 22957510]
54. Givaja G, Amo-Ochoa P, Gomez-Garcia CJ, Zamora F. Chem. Soc. Rev. 2012; 41:115. [PubMed: 21713280]
55. a) Okubo T, Tanaka N, Kim KH, Anma H, Seki S, Saeki A, Maekawa M, Kuroda-Sowa T. Dalton Trans. 2011; 40:2218. [PubMed: 21180735] b) Zhao Y, Hong M, Liang Y, Cao R, Li W, Weng J, Lu S. Chem. Commun. 2001:1020.c) Su W, Hong M, Weng J, Cao R, Lu S. Angew. Chem. Int. Ed. 2000; 39:2911.d) Dirk CW, Bousseau M, Barrett PH, Moraes F, Wudl F, Heeger AJ. Macromolecules. 1986; 19:266.e) Arumugam K, Shaw MC, Chandrasekaran P, Villagran D, Gray TG, Mague JT, Donahue JP. Inor. Chem. 2009; 48:10591.f) Turner DL, Vaid TP, Stephens PW, Stone KH, DiPasquale AG, Rheingold AL. J. Am. Chem. Soc. 2008; 130:14. [PubMed: 18067299]

g) Szczepura LF, Galloway CP, Zheng YF, Han PD, Rheingold AL, Wilson SR, Rauchfuss TB. Angew. Chem.-Int. Edit. 1995; 34:1890.

56. Takaishi S, Hosoda M, Kajiwara T, Miyasaka H, Yamashita M, Nakanishi Y, Kitagawa Y, Yamaguchi K, Kobayashi A, Kitagawa H. Inor. Chem. 2008; 48:9048.
57. a) Acker DS, Harder RJ, Hertler WR, Mahler W, Melby LR, Benson RE, Mochel WE. J. Am. Chem. Soc. 1960; 82:6408.b) Aumuller A, Erk P, Klebe G, Hunig S, Vonschutz JU, Werner HP. Angew. Chem.-Int. Edit. 1986; 25:740.c) Heintz RA, Zhao HH, Xiang OY, Grandinetti G, Cowen J, Dunbar KR. Inor. Chem. 1999; 38:144.
58. a) Bousseau M, Valade L, Legros JP, Cassoux P, Garbauskas M, Interrante LV. J. Am. Chem. Soc. 1986; 108:1908.b) Qin Y-R, Zhu Q-Y, Huo L-B, Shi Z, Bian G-Q, Dai J. Inor. Chem. 2010; 49:7372.c) Nguyen TLA, Demir-Cakan R, Devic T, Morcrette M, Ahnfeldt T, Auban-Senzier P, Stock N, Goncalves A-M, Filinchuk Y, Tarascon J-M, F900E9;rey Gr. Inor. Chem. 2010; 49:7135.
59. a) Behera JN, D'Alessandro DM, Soheilnia N, Long JR. Chem. Mater. 2009; 21:1922.b) Allendorf MD, Schwartzberg A, Stavila V, Talin AA. Chem. Eur. J. 2011; 17:11372. [PubMed: 21932243] c) Wessells CD, Huggins RA, Cui Y. Nat. Commun. 2011; 2:550. [PubMed: 22109524] d) Wessells CD, Peddada SV, Huggins RA, Cui Y. Nano Lett. 2011; 11:5421. [PubMed: 22043814]
60. Wiers BM, Foo M-L, Balsara NP, Long JR. J. Am. Chem. Soc. 2011; 133:14522. [PubMed: 21877685]
61. a) Kreuer KD. Chem. Mater. 1996; 8:610.b) Li QF, He RH, Jensen JO, Bjerrum NJ. Chem. Mater. 2003; 15:4896.c) Hogarth WHJ, da Costa JCD, Lu GQ. J. Power Sources. 2005; 142:223.d) Paschos O, Kunze J, Stimming U, Maglia F. J. Phys. Condens. Matter. 2011:23.
62. Kitagawa H, Nagao Y, Fujishima M, Ikeda R, Kanda S. Inor. Chem. Commun. 2003; 6:346.
63. a) Sadakiyo M, Yamada T, Kitagawa H. J. Am. Chem. Soc. 2009; 131:9906. [PubMed: 19621952] b) Okawa H, Shigematsu A, Sadakiyo M, Miyagawa T, Yoneda K, Ohba M, Kitagawa H. J. Am. Chem. Soc. 2009; 131:13516. [PubMed: 19715318] c) Sadakiyo M, Okawa H, Shigematsu A, Ohba M, Yamada T, Kitagawa H. J. Am. Chem. Soc. 2012; 134:5472. [PubMed: 22409393] d) Taylor JM, Mah RK, Moudrakovski IL, Ratcliffe CI, Vaidhyanathan R, Shimizu GKH. J. Am. Chem. Soc. 2010; 132:14055. [PubMed: 20857972] e) Sahoo SC, Kundu T, Banerjee R. J. Am. Chem. Soc. 2011; 133:17950. [PubMed: 21919488] f) Bureekaew S, Horike S, Higuchi M, Mizuno M, Kawamura T, Tanaka D, Yanai N, Kitagawa S. Nat. Mater. 2009; 8:831. [PubMed: 19734885] g) Hurd JA, Vaidhyanathan R, Thangadurai V, Ratcliffe CI, Moudrakovski IL, Shimizu GKH. Nat. Chem. 2009; 1:705. [PubMed: 21124357] h) Shigematsu A, Yamada T, Kitagawa H. J. Am. Chem. Soc. 2011; 133:2034. [PubMed: 21284399]
64. Gust D, Moore TA, Moore AL. Acc. Chem. Res. 2009; 42:1890. [PubMed: 19902921]
65. Son H-J, Jin S, Patwardhan S, Wezenberg SJ, Jeong NC, So M, Wilmer CE, Sarjeant AA, Schatz GC, Snurr RQ, Farha OK, Wiederrecht GP, Hupp JT. J. Am. Chem. Soc. 2012; 135:862. [PubMed: 23249338]
66. Wang C, Wang J-L, Lin W. J. Am. Chem. Soc. 2012; 134:19895. [PubMed: 23136923]
67. Wang C, deKrafft KE, Lin W. J. Am. Chem. Soc. 2012; 134:7211. [PubMed: 22486151]
68. Chen B, Wang L, Xiao Y, Fronczek FR, Xue M, Cui Y, Qian G. Angew. Chem. Int. Ed. 2009; 48:500.
69. Rieter WJ, Taylor KML, Lin WB. J. Am. Chem. Soc. 2007; 129:9852. [PubMed: 17645339]
70. Thomas SW, Joly GD, Swager TM. Chem. Rev. 2007; 107:1339. [PubMed: 17385926]
71. Kent CA, Liu D, Meyer TJ, Lin W. J. Am. Chem. Soc. 2012; 134:3991. [PubMed: 22329430]
72. Wanderley MM, Wang C, Wu C-D, Lin W. J. Am. Chem. Soc. 2012; 134:9050. [PubMed: 22607498]
73. Halder GJ, Kepert CJ, Moubaraki B, Murray KS, Cashion JD. Science. 2002; 298:1762. [PubMed: 12459583]
74. a) Li B, Wei RJ, Tao J, Huang RB, Zheng LS, Zheng ZP. J. Am. Chem. Soc. 2010; 132:1558. [PubMed: 20085322] b) Nihei M, Han LQ, Oshio H. J. Am. Chem. Soc. 2007; 129:5312. [PubMed: 17417846] c) Neville SM, Halder GJ, Chapman KW, Duriska MB, Southon PD, Cashion JD, Letard JF, Moubaraki B, Murray KS, Kepert CJ. J. Am. Chem. Soc. 2008; 130:2869. [PubMed: 18254628] d) Neville SM, Moubaraki B, Murray KS, Kepert CJ. Angew. Chem. Int. Ed. 2007; 46:2059.

75. a) Al-Jamal WT, Kostarelos K. Acc. Chem. Res. 2011; 44:1094. [PubMed: 21812415] b) Namiki Y, Fuchigami T, Tada N, Kawamura R, Matsunuma S, Kitamoto Y, Nakagawa M. Acc. Chem. Res. 2011; 44:1080. [PubMed: 21786832]
76. Oh M, Mirkin CA. Nature. 2005; 438:651. [PubMed: 16319888]
77. a) Lin W, Rieter WJ, Taylor KM. Angew. Chem. Int. Ed. 2009; 48:650.b) Della Rocca J, Lin WB. Eur. J. Inorg. Chem. 2010:3725.
78. Taylor, Kathryn ML.; Jin, A.; Lin, W. Angew. Chem. Int. Ed. 2008; 47:7722.
79. a) Horcajada P, Serre C, Vallet-Regí M, Sebban M, Taulelle F, Férey G. Angew. Chem. Int. Ed. 2006; 45:5974.b) An J, Geib SJ, Rosi NL. J. Am. Chem. Soc. 2009; 131:8376. [PubMed: 19489551]
80. a) deKrafft KE, Boyle WS, Burk LM, Zhou OZ, Lin W. J. Mater. Chem. 2012; 22:18139. [PubMed: 23049169] b) Della Rocca J, Huxford RC, Comstock-Duggan E, Lin W. Angew. Chem. Int. Ed. 2011; 50:10330.
81. a) Rowe MD, Thamm DH, Kraft SL, Boyes SG. Biomacromolecules. 2009; 10:983. [PubMed: 19290624] b) Hatakeyama W, Sanchez TJ, Rowe MD, Serkova NJ, Liberatore MW, Boyes SG. ACS App. Mater. & Interface. 2011; 3:1502.
82. Maeda H, Matsumura Y. Adv. Drug Deliver. Rev. 2011; 63:129.

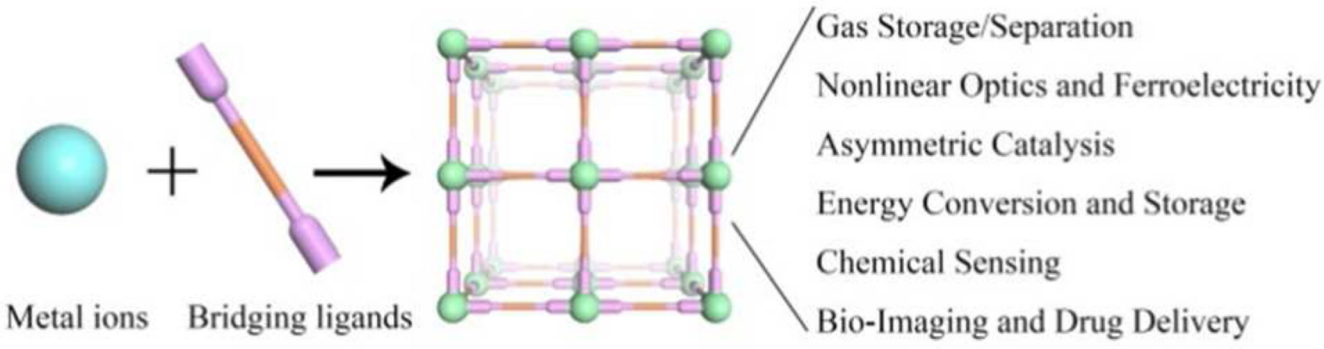

Figure 1.
Synthesis of functional MOFs for various applications.

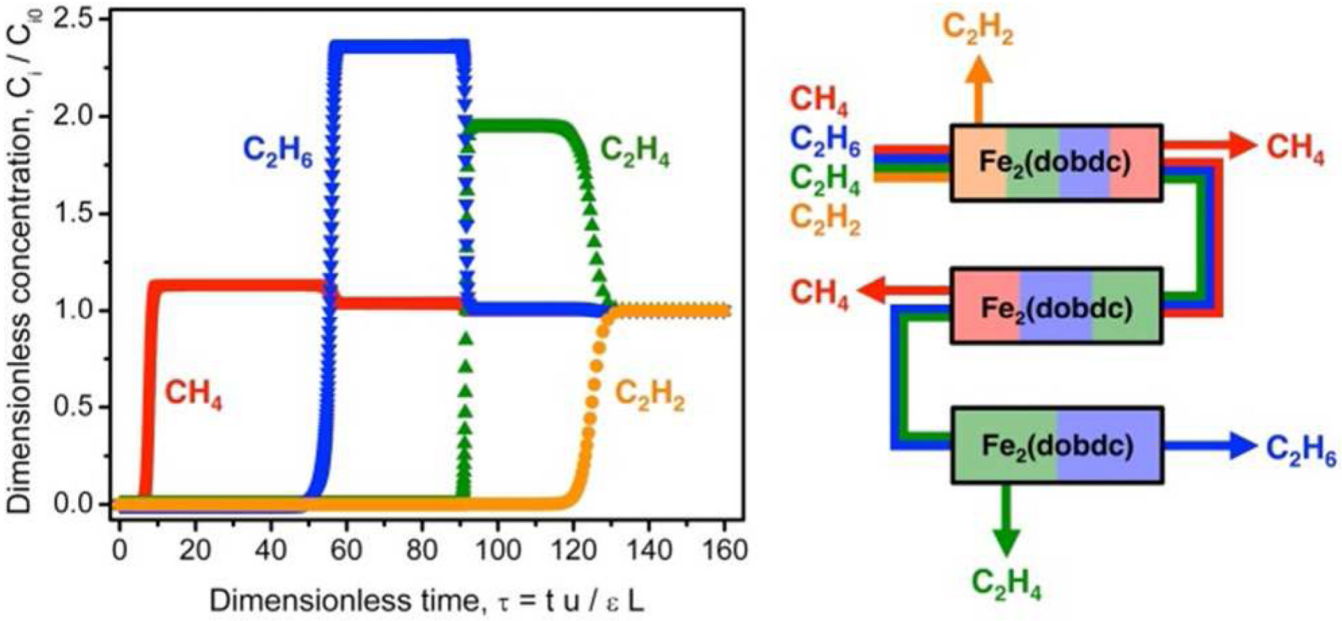

Figure 2.

Left, calculated methane (red), ethane (blue), ethylene (green) and acetylene (orange) breakthrough curves for an equimolar mixture of the gases at 1 bar flowing through a fixed bed of Fe_2(DOBDC) at 318K. Right, schematic representation of the separation of a mixture of methane, ethane, ethylene, and acetylene using three packed beds of Fe_2(DOBDC) in a vacuum swing adsorption or temperature swing adsorption process. Reproduced with permission from reference [34]. Copyright: Science Magazine 2012.

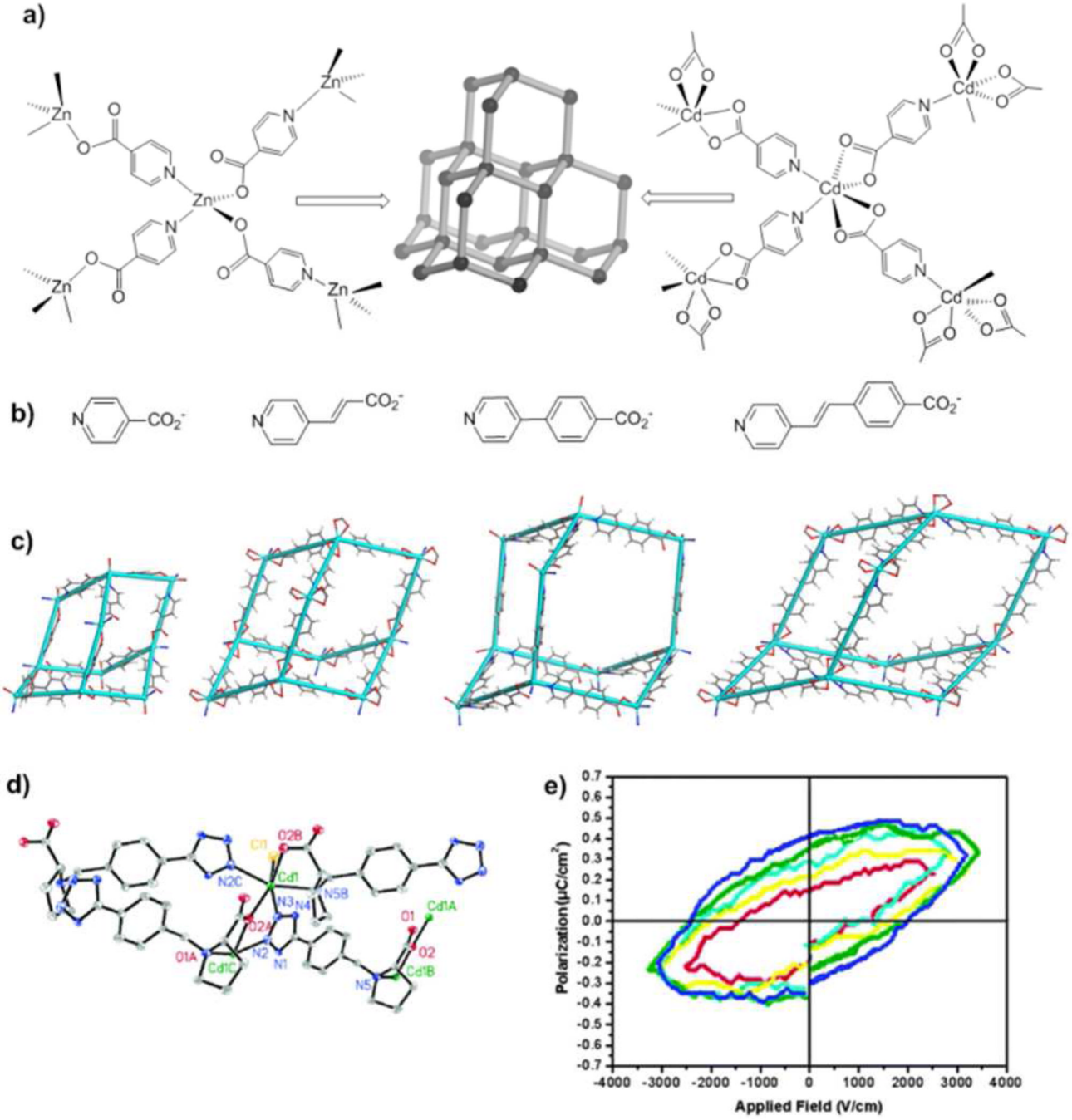

Figure 3.

a) Construction of MOFs with 3-D diamond structures from a linear pyridinecarboxylate ligand and Zn^{2+}/Cd^{2+} nodes. b) Structures of linear pyridinecarboxylate ligands. c) Diamondoid structures built from linear pyridinecarboxylate ligands. d) Asymmetric unit of the crystal of Cd-TBP. e) Electric field polarization cycles of Cd-TBP. d) and e) reproduced with permission from reference [39c]. Copyright: American Chemical Society 2006.

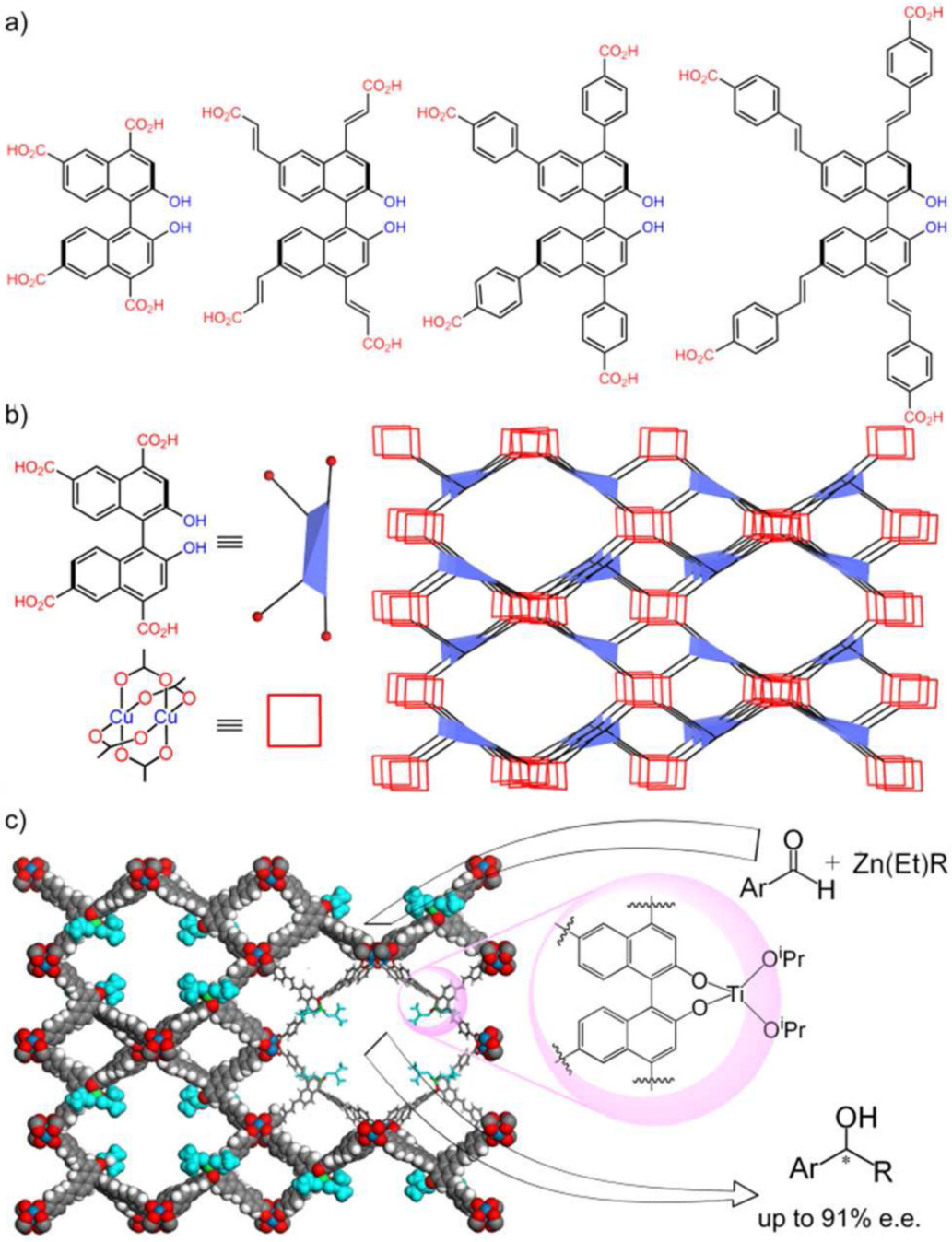

Figure 4.

a) Chemical structures of BINOL-derived tetracarboxylic acid ligands (BINOL-TC). b) Representation of the BINOL-TC ligand as a blue distorted tetrahedron and the $[Cu_2(O_2CR)_4]$ paddlewheel as a red square, and simplified connectivity scheme of the MOF structure. c) Schematic representation of asymmetric alkyl- and alkynylzinc additions catalyzed by the MOF-based Ti-BINOLate catalyst within large open channels. Reproduced with permission from reference [16f]. Copyright: Nature Publishing Group 2010.

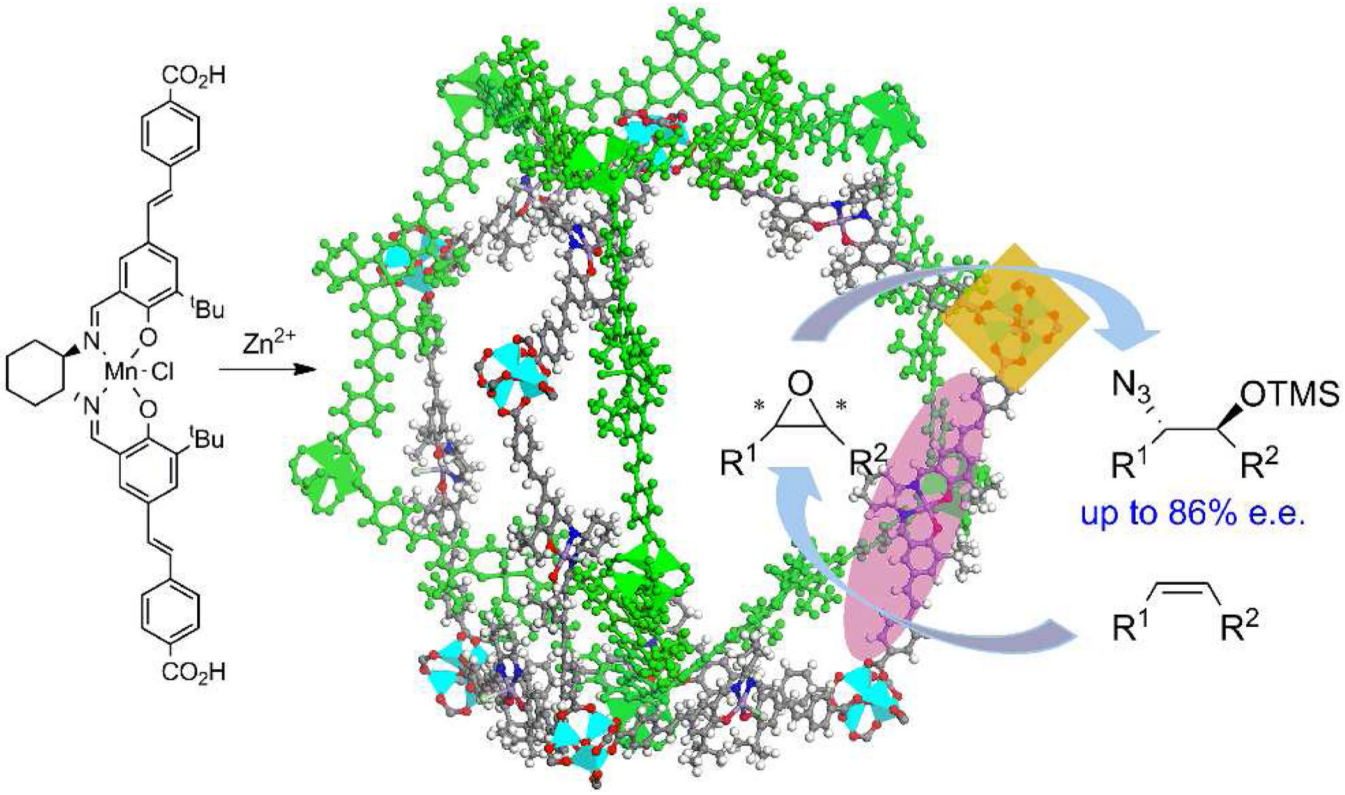

Figure 5.
Schematic representation of sequential asymmetric epoxidation and ring-opening reactions catalyzed by the Mn-Salen-based ligand and $[Zn_4(\mu_4\text{-}O)(CO_2)_6]$ SBU, respectively. Reproduced with permission from reference [16g]. Copyright: Royal Society of Chemistry 2011.

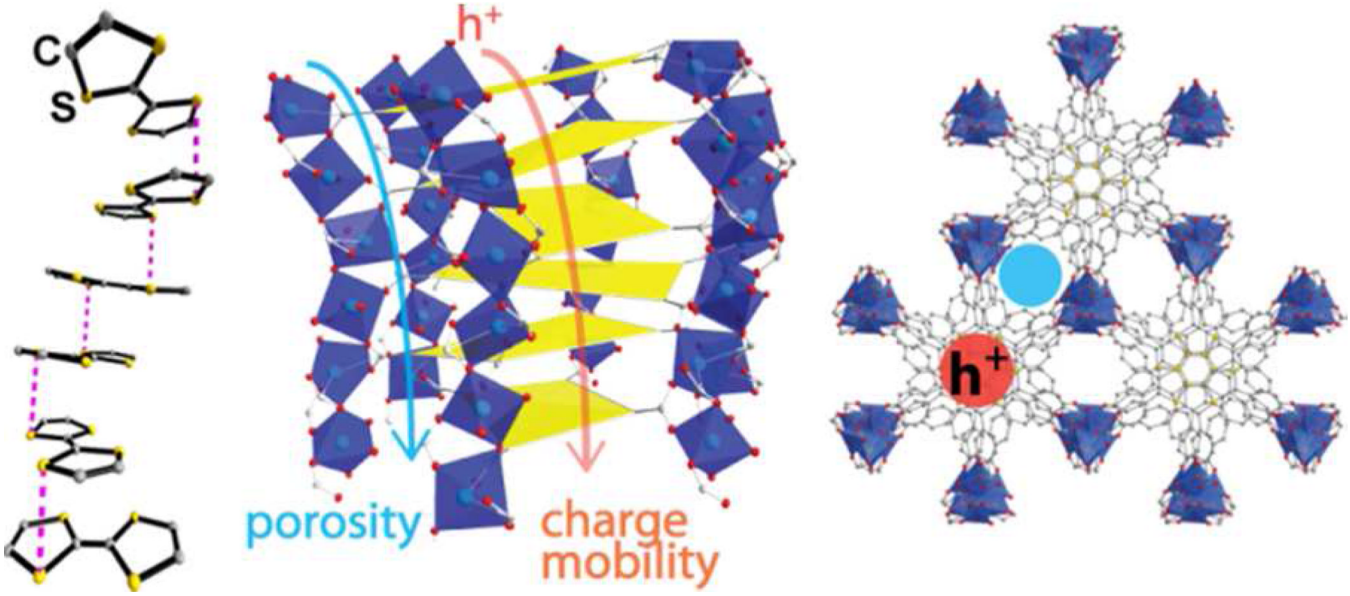

Figure 6.

Left, electron transport pathway through a continuum of TTF moiety in the crystal structure of Zn_2(TTFTB). Middle and right, crystal structure of Zn_2(TTFTB) showing porosity and charge transport through parallel channels. Reproduced with permission from reference [12d]. Copyright: American Chemical Society 2012.

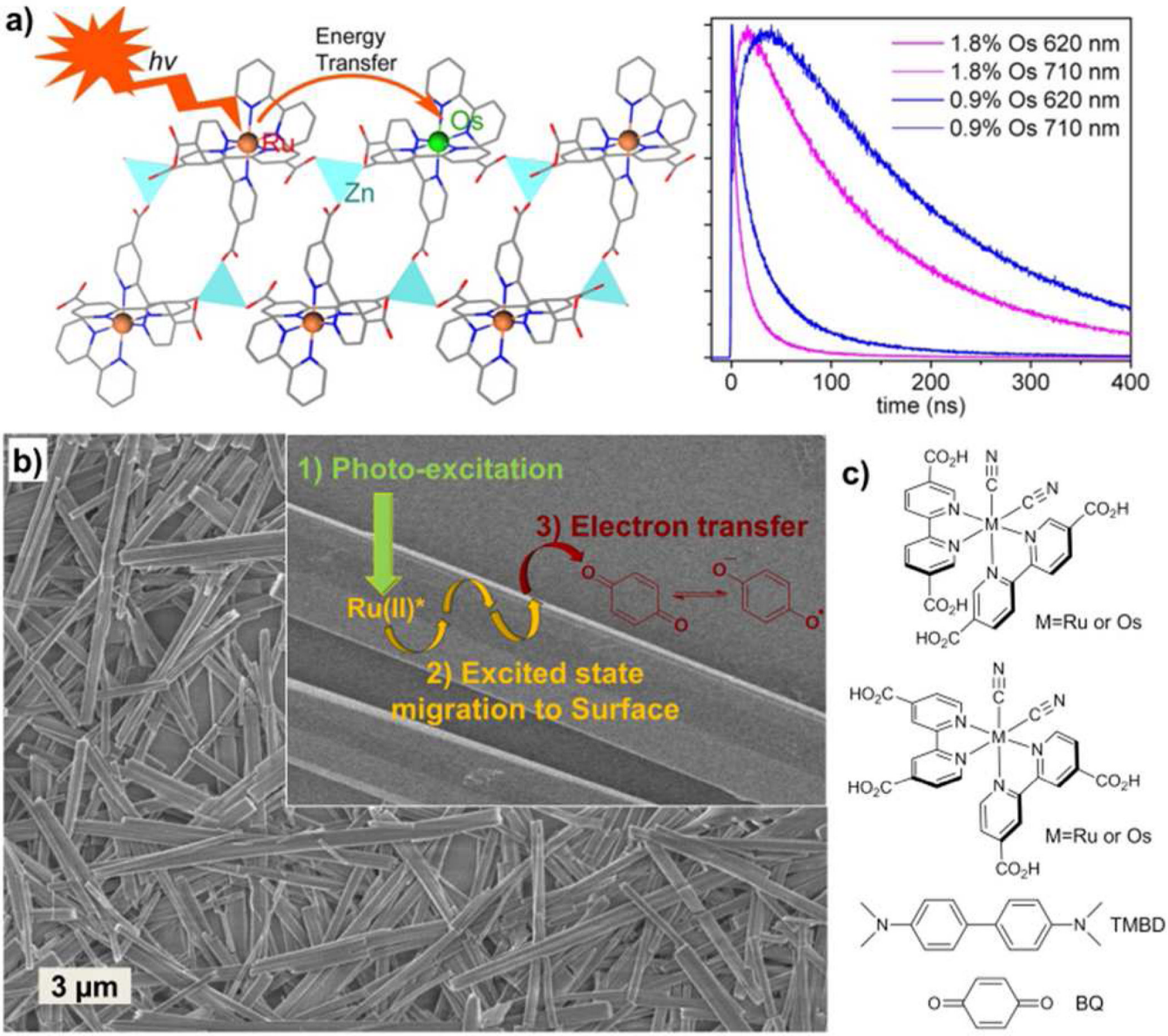

Figure 7.

a) Schematic showing energy transfer in a MOF crystal (left) and decay transients of $Ru(bipy)_3^{2+*}$ and $Os(bipy)_3^{2+*}$ in Os-doped MOFs built from $Ru(bipy)_3^{2+}$ derivatives (right). b) Light-harvesting with a MOF microcrystal. The ^{3}MLCT excited states undergo rapid intra-framework energy migration to carry out electron transfer quenching at the MOF/solution interface. c) Chemical structures of the photoactive MOF building blocks and reductive tetramethylbenzidine (TMBD) and oxidative benzoquione (BQ) quenchers. Reproduced with permission from references [19a] (a) and [19b] (b and c). Copyright: American Chemical Society 2009 and 2010.

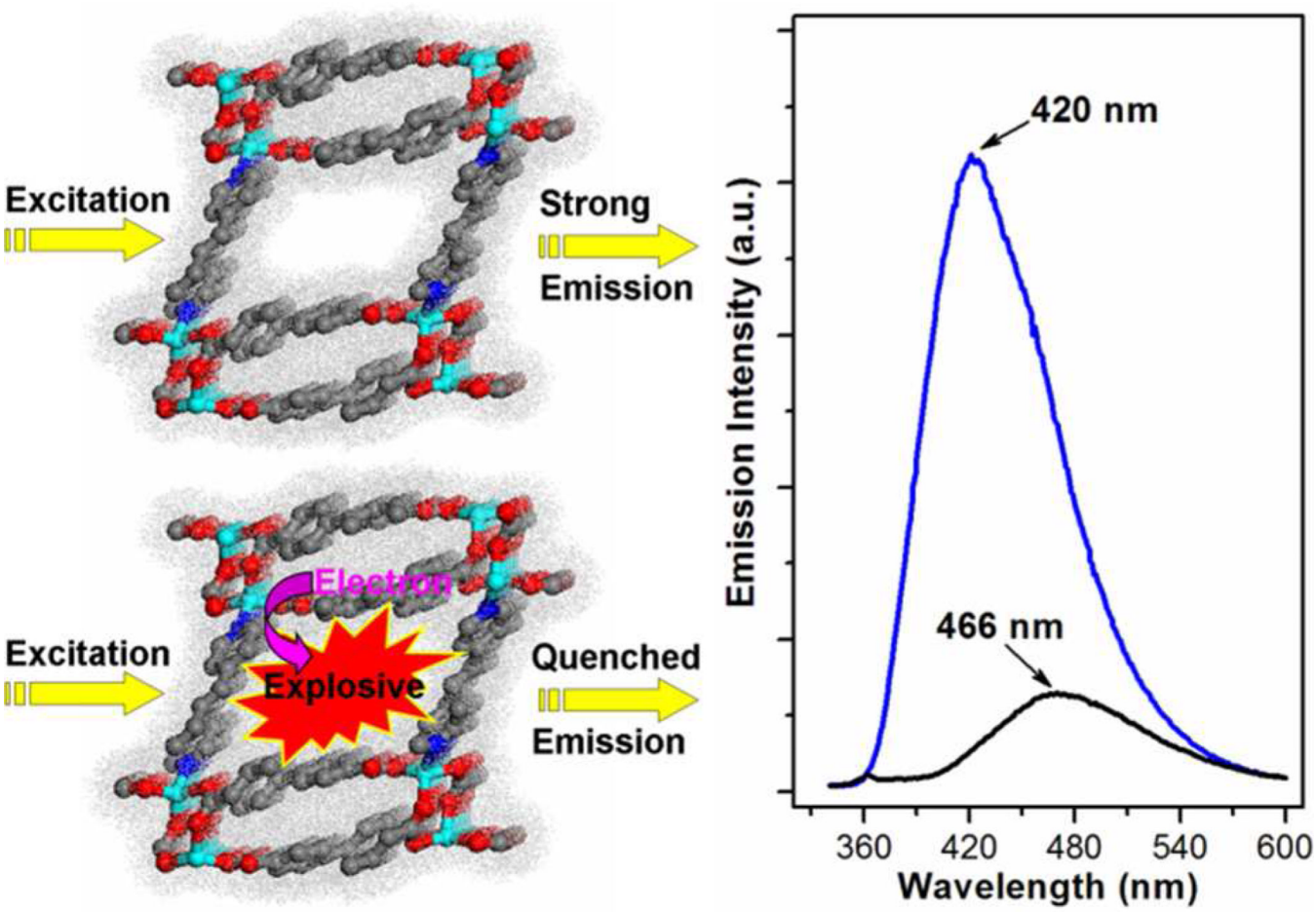

Figure 8.

Luminescent quenching of $[Zn_2(bpdc)_2(bpee)]$ by vapor of solid explosives DNT and DMNB for explosive detection. Reproduced with permission from reference [15b]. Copyright: Wiley 2009.

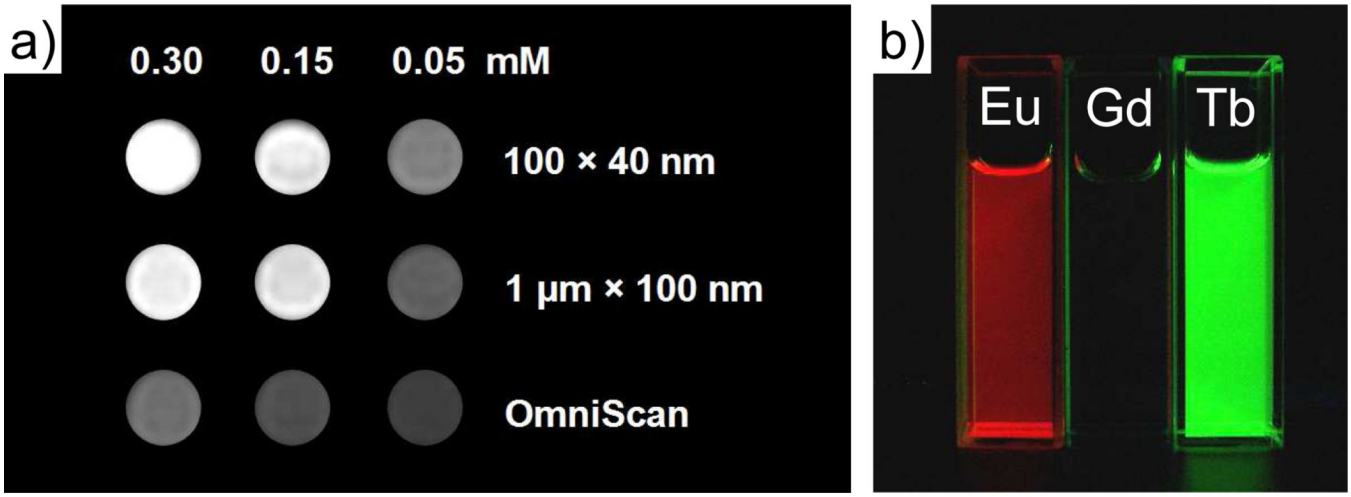

Figure 9.

a) T_1-weighted MR phantom images of suspensions of $Gd(BDC)_{1.5}(H_2O)_2$ in water containing 0.1 % xanthan gum as a dispersing agent. b) Luminescence of ethanolic dispersions of Eu- and Tb-doped $Gd(BDC)_{1.5}(H_2O)_2$ when irradiated with UV light.

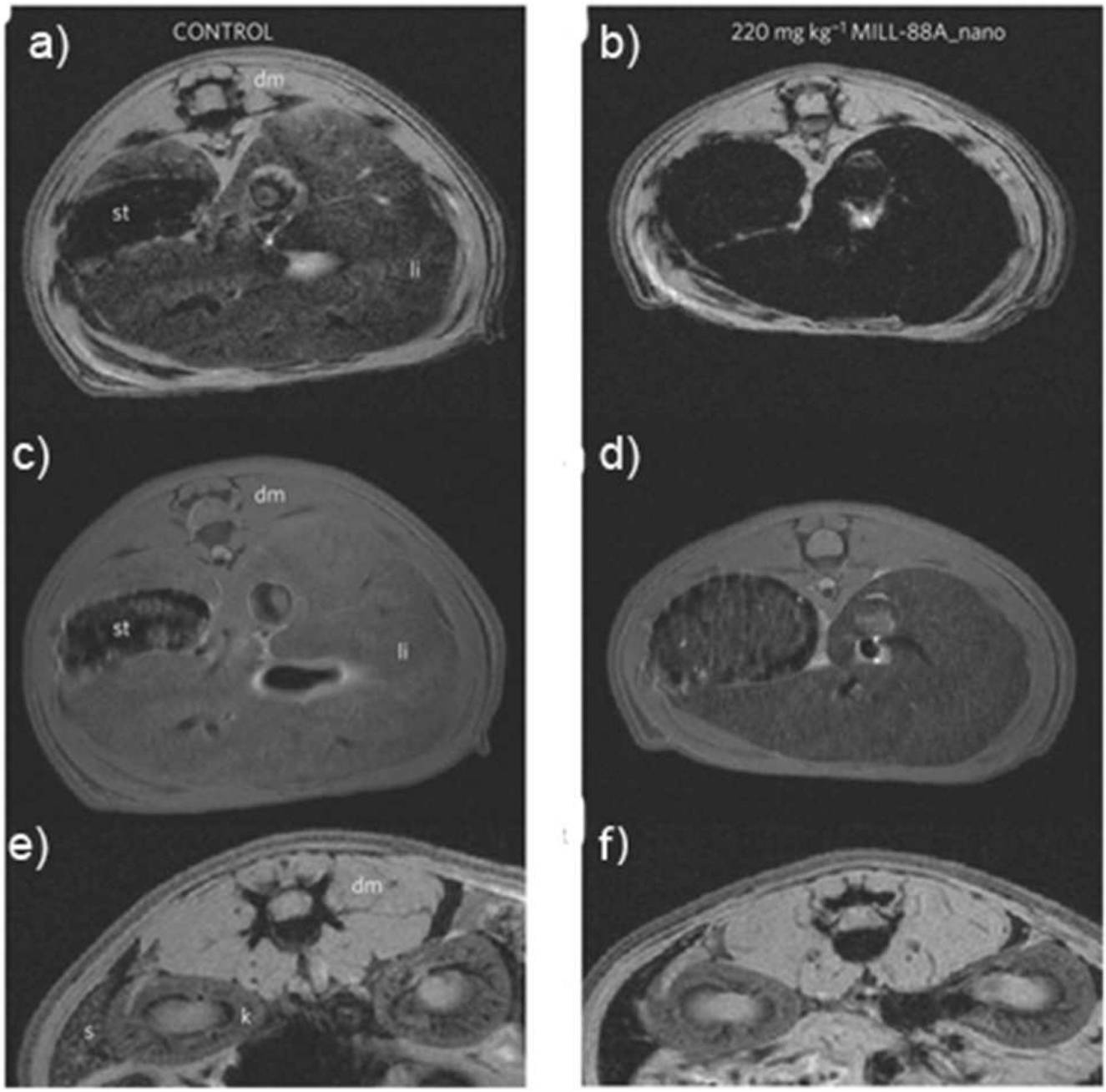

Figure 10.

T_2 weighted MR images of Wistar rats injected with no particle (a,c,e) or 220 mg/kg MIL-88A (e,d,f). The images were acquired using either gradient echo (a,b,e,f) or spin echo (c,d) sequences. The images show the liver (a–d) or spleen (e,f) regions 30 minutes post-injection. [dm=dorsal muscle, k=kidney, li=liver, s=spleen, st=stomach]. Reproduced with permission from reference [18a]. Copyright: Nature Publishing Group 2010.

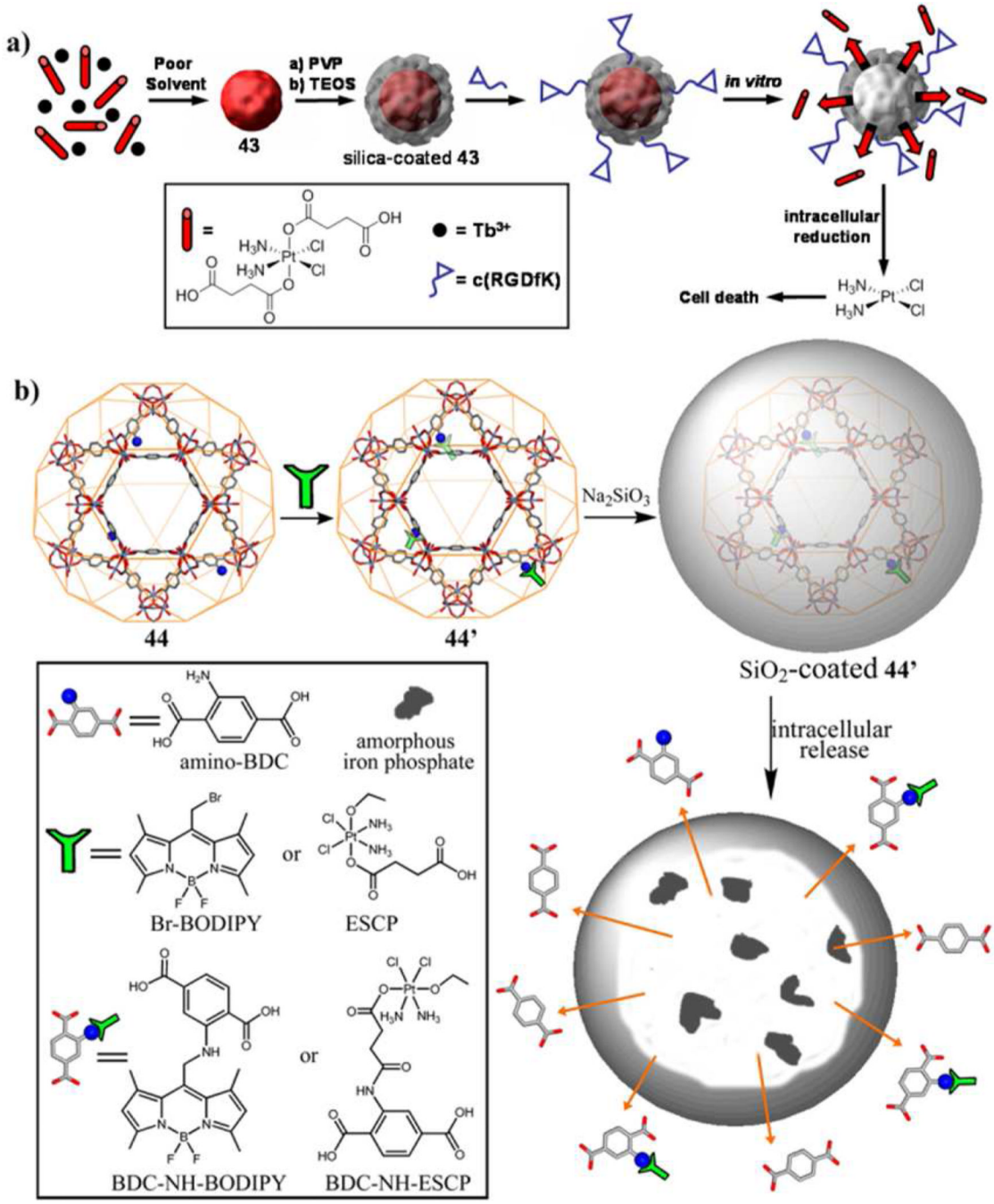

Figure 11.

Left) SEM image of MIL-101. The inset shows the 42@silica@PEG particles. Right) Confocal microscopy image of H460 cells that have been incubated with MIL-101@SiO_2-PEG-AA. Reproduced with permission from reference [18c]. Copyright: American Chemical Society 2009.

J Am Chem Soc. Author manuscript; available in PMC 2014 September 11.

Table 1

Selected Examples of MOFs with highest gas uptake capacities.

MOF	BET Surface area (m^2/g)	Pore volume (cm^3g^{-1})	Pressure (bar)	Excess H_2 uptake at 77 K (wt%)/Volumetric (g/L)	Excess H_2 uptake at 298 K (wt%)	Excess CH_4 uptake at 298 K (wt %)/Volumetric (g/L)
Zn-TBCPPM[23]	2718	1.46	80	5.8/39	1.6	27.6/189
MOF-200[21c]	4530	3.59	80	7.4/36	0.28	23.4/114
MOF-205[21c]	4460	2.16	80	7.0/46	NA	25.8/167
MOF-210[21c]	6240	3.6	80	8.6/44	NA	26.4/135
MOF-177[29]	4526	1.59	70	7.5/32	NA	NA
NOTT-112[30]	3800	1.62	35	7.07/35.6	NA	NA
NOTT-140[22a]	2620	1.07	20	6.0/41[a]	NA	15.3[c]/105
UTSA-20[22b]	1156	0.63	15	4.1/36	NA	14[d]/123
PCN-14[22c]	1753	0.87	45	4.42/36.6	NA	18[e]/149
PCNP-66[22d]	4000	1.63	45	6.65/29.6	0.785[b]	17.5[d]/78
PCN-68[22d]	5109	2.13	50	7.32/28	1.01[b]	18.6[d]/71
NU-100[21b]	6143	2.82	70	9.95/29	NA	NA
Cu-TDPA[22e]	1938	0.93	52	4.89/38	0.61[f]	16.8[g]/131
Mn-BTT[31]	2100	0.795	90	5.1/43	0.94	NA
SNU-77H[22f]	3670	1.52	90	8.1/47.4	0.5	17.7[h]/104
FJI-1[22g]	4043	1.21	62	6.52/26.4	0.43	24.5/99

[a] total uptake.

[b] 90 bar.

[c] 293 K.

[d] 35 bar.

[e] 290 K, 35 bar

[f] 61 bar.

[g] 80 bar.

$h_{60\ \text{bar.}}$